# The Parkinson's gene PINK1 activates Akt via PINK1 kinase-dependent regulation of the phospholipid PI(3,4,5)$P_3$

**Authors:** Rachel M. Furlong [a, b, c], Andrew Lindsay [a], Karen E. Anderson [d], Phillip T. Hawkins [d], Aideen M. Sullivan [b, c, #], and Cora O'Neill [a, c, #, 1]

**Affiliations:**

[a] School of Biochemistry and Cell Biology, Biosciences Institute, University College Cork, Cork City, T12 YT20, Ireland. a.lindsay@ucc.ie

[b] Department of Anatomy and Neuroscience, Western Gateway Building, University College Cork, Cork City, T12 XF62, Ireland. a.sullivan@ucc.ie

[c] Cork NeuroScience Centre, University College Cork, Cork City, T12 YT20, Ireland.

[d] Signalling Programme, Babraham Institute, Cambridge, CB22 3AT, UK. karen.anderson@babraham.ac.uk, phillip.hawkins@babraham.ac.uk

[#] These authors contributed equally to this work

[1] Corresponding author:

Tel: +353 21 4901380; Fax: + 353 21 4901382; Email: c.oneill@ucc.ie

**Keywords:**

Akt / Parkinson's disease / PINK1 / PI(3,4,5)$P_3$ ($PIP_3$)



JCS Advance Online Article. Posted on 20 September 2019

**Summary statement:**

Loss of PINK1 kinase function as occurs in Parkinson's disease, causes impaired activation of Akt, as a result of defects in phospholipid PI(3,4,5)$P_3$ regulation.

**Abstract:**

Akt signalling is central to cell survival, metabolism, protein and lipid homeostasis, and is impaired in Parkinson's disease(PD). Akt activation is reduced in the PD brain, and by many PD-causing genes, including PINK1(PTEN-induced putative kinase-1). This study investigated the mechanisms by which PINK1 regulates Akt signalling. Our results reveal for the first time that PINK1 constitutively activates Akt in a PINK1-kinase dependent manner in the absence of growth factors, and enhances Akt activation in normal growth medium. In PINK1 modified MEFs, agonist-induced Akt signalling failed in the absence of PINK1, due to significantly impaired PINK1 kinase-dependent increases in PI(3,4,5)$P_3$ at both plasma membrane and Golgi. In the absence of PINK1, PI(3,4,5)$P_3$ levels did not increase in the Golgi, and there was significant Golgi fragmentation, a recognised characteristic of PD neuropathology. PINK1 kinase activity protected the Golgi from fragmentation in an Akt-dependent fashion. This study demonstrates a new role for PINK1 as a primary upstream activator of Akt via PINK1 kinase-dependent regulation of its primary activator PI(3,4,5)$P_3$, providing novel mechanistic information on how loss of PINK1 impairs Akt signalling in PD.

**Introduction:**

*PINK1* (phosphatase and tensin homologue (PTEN)-induced kinase 1) was identified as a gene upregulated by overexpression of the tumor suppressor PTEN, the major negative regulator of phosphoinositide-3-kinase (PI3-kinase)/Akt signalling (Unoki and Nakamura, 2001). Subsequently, loss of function mutations in *PINK1* were reported to cause autosomal recessive early onset Parkinson's disease (PD) (Valente et al., 2004), leading to a major research effort to understand PINK1 function. PINK1, a ubiquitous serine-threonine kinase, has pro-survival, neuroprotective and anti-stress signalling functions (Arena et al., 2013, Haque et al., 2008, Li et al., 2017, MacKeigan et al., 2005, Wood-Kaczmar et al., 2008, Yang et al., 2018). Multiple studies, from our and other labs, have shown that PINK1 is a key regulator of mitochondrial health, including mitophagy, fission, fusion, bioenergetics and mitochondrial antigen presentation (Harper et al., 2018, Matheoud et al., 2016, O'Flanagan et al., 2015, Pilsl and Winklhofer, 2012, Youle and Narendra, 2011, Youle and van der Bliek, 2012). Although these are the most widely documented functions of PINK1, PINK1 also regulates several other non-mitochondrial systems central to survival, neuroprotection and stress-resistance (Dagda et al., 2009, Dagda et al., 2014, Dickey and Strack, 2011, Fedorowicz et al., 2014, Ries et al., 2006, Steer et al., 2015, Xiong et al., 2009), for review (Arena and Valente, 2017, O'Flanagan and O'Neill, 2014). These include PI3-kinase/Akt signalling (Akundi et al., 2012, Contreras-Zarate et al., 2015, Ellis et al., 2013, Maj et al., 2010, Sanchez-Mora et al., 2012), the cell cycle (O'Flanagan et al., 2015), protein kinase A (Dagda et al., 2014, Dickey and Strack, 2011), NF-κB (Lee and Chung, 2012, Lee et al., 2012, Sha et al., 2010), ubiquitination, proteasomal degradation (Xiong et al., 2009) and macroautophagy (Dagda et al., 2009, Fedorowicz et al., 2014).

Understanding the interactions between PINK1 and the PI3-kinase/Akt pathway is of central importance for PD research, as this pathway is a master regulator of cell survival, metabolism and proteostasis, key systems that fail in PD (Manning and Toker, 2017). In concordance, Akt activation is impaired in postmortem tissue from the substantia nigra of PD patients (Malagelada et al., 2008, Timmons et al., 2009), and constitutive activation of Akt protects against dopaminergic neuron loss in a preclinical model of PD (Ries et al., 2006). Notably, several PD risk genes, including PINK1, converge to crosstalk with the PI3-kinase/Akt signalling system (Chuang et al., 2014, Fallon et al., 2006, Gupta et al., 2017, Jaramillo-Gomez et al., 2015, Kim et al., 2005, Ohta et al., 2011, Zhang et al., 2016). Akt activation by PINK1 confers protection against several cell stressors including rotenone (Murata et al.,

2011), calyculin A, FK506, staurosporine (Akundi et al., 2012), and ceramide (Contreras-Zarate et al., 2015, Sanchez-Mora et al., 2012). Akt-induced inhibition of FOXO3a can reduce PINK1 mRNA levels (Mei et al., 2009), and Akt signalling regulates PINK1-dependent mitophagy (Deas et al., 2011, Hauser et al., 2017, Matsuda et al., 2010, McCoy et al., 2014, Soutar et al., 2018).

Akt activation mechanisms and Akt signalling are the subject of intensive investigation in cell biology in health and disease, (Manning and Toker, 2017) for review. Accumulation of the membrane lipid phosphatidylinositol (3,4,5)-trisphosphate ($PI(3,4,5)P_3$ or $PIP_3$), via agonist-induced PI3-kinase phosphorylation of $PI(4,5)P_2$, is an essential prerequisite for Akt activation. $PIP_3$ acts by recruiting inactive cytosolic Akt to membranes by interacting with its pleckstrin homology (PH) domain (Bellacosa et al., 1998). This interaction induces a conformational change in Akt, essential for Akt activation, allowing phosphorylation at two regulatory residues, $Ser^{473}$ by mammalian target of rapamycin complex 2 (mTORC2) (Alessi et al., 1996, Sarbassov et al., 2005, Stokoe et al., 1997), and $Thr^{308}$, by phosphoinositide dependent kinase 1 (PDK1) (Calleja et al., 2007, Stokoe et al., 1997). Termination of PI3-kinase-$PIP_3$-Akt signalling is predominantly due to dephosphorylation of $PIP_3$ to $PI(4,5)P_2$ by the phosphatase PTEN (Maehama and Dixon, 1998, Stokoe et al., 1997). It is increasingly recognised that $PIP_3$ can equilibrate between endomembranes via membrane trafficking routes, and can also be generated within endomembranes *in situ* (Braccini et al., 2015, Ebner et al., 2017, Jethwa et al., 2015, Salamon and Backer, 2013, Sato et al., 2003). The observation that Akt localises to endomembranes, in addition to the plasma membrane, has led to the modification of Akt signalling models to incorporate compartment-specific patterns of activation (Ebner et al., 2017, Manning and Toker, 2017).

While it is clear that PINK1 can activate Akt (Akundi et al., 2012, Boonying et al., 2019, Contreras-Zarate et al., 2015, Ellis et al., 2013, Hauser et al., 2017, Maj et al., 2010, Mei et al., 2009, Murata et al., 2011, O'Flanagan and O'Neill, 2014, Sanchez-Mora et al., 2012, Soutar et al., 2018), and that PINK1 deletion reduces Akt activation, the mechanism by which this occurs and its dependence on PINK1 kinase activity remain unclear. Initial studies revealed that PINK1 markedly enhanced the phosphorylation of Akt at $Ser^{473}$ but not $Thr^{308}$, inducing Akt activation that was essential for protection from a variety of cytotoxic agents (Murata et al., 2011). PINK1- induced Akt activation was reported to occur independently of PI3-kinase, via PINK1-mediated activation of mTORC2 via Rictor (Murata et al., 2011). In contrast, subsequent studies revealed that mouse embryonic fibroblasts (MEFs) from PINK1$^-$

$^{-/-}$ mice had reduced IGF-1- and insulin-induced activation of Akt, with reduced phosphorylation at both Akt activation residues, $Thr^{308}$ and $Ser^{473}$, and protection from apoptosis and metabolic dysfunction (Akundi et al., 2012). Together, these studies show that PINK1 promotes Akt activation via a mechanism upstream of Akt phosphorylation (Akundi et al., 2012, Contreras-Zarate et al., 2015, Ellis et al., 2013, Maj et al., 2010, Manning and Toker, 2017, Mei et al., 2009, Murata et al., 2011, Sanchez-Mora et al., 2012). However, various mechanisms have been proposed and there is no clear information on whether Akt activation requires PINK1 kinase activity.

In this study, we employed PINK1-modifed cell systems (Morais et al., 2009, O'Flanagan et al., 2015) to investigate the mechanism by which PINK1 activates Akt. We identify PINK1 as a major upstream activator of Akt, and provide a new mechanism involving PINK1 kinase-dependent regulation of the plasma membrane and endomembrane localisation of $PIP_3$, the essential lipid activator of Akt. This study significantly advances knowledge on the mechanisms by which loss of function of PINK1 impairs Akt activation in PD.

**Results:**

**PINK1 activates Akt in a PINK1 kinase-dependent manner**

Initial results show that terminally-differentiated mouse embryonic fibroblasts (MEFs) derived from $PINK1^{-/-}$ mice (Morais et al., 2009, O'Flanagan et al., 2015) displayed significantly reduced Akt phosphorylation at both $Ser^{473}$ and $Thr^{308}$ activating residues, when cultured in normal growth medium (Fig. 1A). Total Akt levels were equivalent in $PINK1^{-/-}$ and $PINK1^{+/+}$ cells, indicating that deletion of PINK1 significantly reduced activation of Akt (phospho-Akt/Akt ratio). These findings were confirmed in BE(2)-M17 neuroblastoma cells transduced with shRNA to PINK1 (Fig 1B). Stable expression of human PINK1 ($hPINK1_{res}$) in $PINK1^{-/-}$ MEFs fully restored phosphorylation at the $Ser^{473}$ residue ($p < 0.05$), and partially restored phosphorylation at $Thr^{308}$ ($p = 0.09$) (Fig 1A). In contrast, a triple kinase dead PINK1 mutant ($hPINK1_{TKD}$) did not restore phosphorylation at either residue (Fig. 1A). Deletion of PINK1 did not alter Akt 1, 2, 3 isoform levels, however expression of $hPINK1_{TKD}$ resulted in a significant decrease in the level of Akt1, which indicates PINK1 kinase activity can

specifically regulate the levels of Akt1 (Fig. 1C). We further demonstrate that PINK1 overexpression in PINK1$^{-/-}$ MEFs resulted in constitutive activation of Akt at both activating residues, in the absence of serum, whereas Akt activation was markedly impaired in wild type, PINK1$^{-/-}$ and hPINK1$_{TKD}$ mutants (Fig. 1D). Total Akt levels were similar in all cell lines (Fig. 1D). Together, these data show that PINK1 activates Akt by inducing phosphorylation at both the mTORC2-dependent Ser$^{473}$ and PDK1-dependent Thr$^{308}$ activation sites, without affecting Akt isoform levels. Additionally, these results indicate that PINK1 can constitutively activate Akt, even in the absence of serum, and that this requires PINK1 kinase activity.

**Plasma membrane localisation of Akt is enhanced by PINK1 kinase activity**

GFP-Akt-PH transfection allows visualisation of Akt at the plasma membrane (Calleja et al., 2007, Ebner et al., 2017, Meyer et al., 2012), which is known to be critical for Akt activation (Bellacosa et al., 1998). We next examined whether increased Akt activation induced by PINK1 was mechanistically associated with increased recruitment of Akt to the plasma membrane. Our results show that, under normal growth conditions, GFP-Akt-PH was localised to the plasma membrane at a number of focal points, where clear areas with increased GFP-Akt-PH were evident in PINK1$^{+/+}$ and hPINK1$_{res}$ cells, but not in PINK1$^{-/-}$ and hPINK1$_{TKD}$ MEFs (Fig. 2A). This was visualised by analysis of the fluorescence intensity along a line that bisected the cell, where sharp peaks of fluorescence intensity were observed where the line crosses the plasma membrane in PINK1$^{+/+}$ and hPINK1$_{res}$ cells but not in PINK1$^{-/-}$ and hPINK1$_{TKD}$ MEFs (Supp. 1A). The percentage of cells with GFP-Akt-PH at the plasma membrane was quantified, revealing a significant reduction in PINK1$^{-/-}$ and hPINK1$_{TKD}$ MEFs ($p < 0.0001$) in comparison to PINK1$^{+/+}$ and hPINK1$_{res}$ MEFs (Fig. 2B).

This impairment in GFP-Akt-PH localisation to the plasma membrane was also evident in PINK1$^{-/-}$ and hPINK1$_{TKD}$ cells in response to the agonist IGF-1, a major activator of Akt (Fig. 3). In unstimulated cells, GFP-Akt-PH was distributed diffusely throughout the cytoplasm in all four MEF cell lines (Fig. 3A). After 2-min stimulation with IGF-1, a rapid and significant increase in the percentage of cells with GFP-Akt-PH at the plasma membrane was evident in both PINK1$^{+/+}$ and hPINK1$_{res}$ MEFs. This was significantly lower ($p < 0.0001$), remaining at baseline levels, in both PINK1$^{-/-}$ or hPINK1$_{TKD}$ MEFs (Fig. 3A,B). The percentage of cells displaying plasma membrane localisation of GFP-Akt-PH in the PINK1$^{-/-}$ and hPINK1$_{TKD}$

cells increased following 10-min IGF-1 stimulation, but remained significantly lower than that observed in PINK1$^{+/+}$ and hPINK1$_{res}$ MEFs cell lines (p = 0.0002) (Fig. 3B). Plasma membrane localisation of full length GFP-Akt is also enhanced by PINK1 kinase activity in the same manner, verifying that this is not due to truncation of Akt (Supp. 2). Thus, it can be concluded that the localisation of Akt at the plasma membrane, which is known to be critical for Akt activation, is regulated by PINK1 kinase activity, both under normal growth conditions and in response to short-term stimulation with IGF-1.

**PI3-kinase p85α subunit phosphorylation is reduced in the absence of PINK1 kinase activity**

Next we sought to identify mechanisms by which PINK1 activates Akt. Firstly we determined whether PINK1 regulated Akt activity by enhancing either PDK1- and /or mTORC2- induced phosphorylation of Akt$^{Thr308}$ and Akt$^{Ser473}$, respectively. PDK1 activation was assessed indirectly by measuring PDK-1$^{Ser241}$ phosphorylation (necessary for PDK-1 activation (Casamayor et al., 1999, Komander et al., 2005, Wick et al., 2003)), SGK-1 (protein downstream of PDK-1 and regulated by its activation (Castel et al., 2016, Hall et al., 2012)) and mTORC2 via Rictor levels (Sarbassov et al., 2004). Comparative western immunoblot analysis revealed there was no significant alteration in PDK1$^{Ser241}$, SGK-1 or Rictor levels when comparing wild-type, PINK1$^{-/-}$, hPINK1$_{res}$ or hPINK1$_{TKD}$ cells (Fig. 4A).

Phosphatidylinositol (3,4,5)-trisphosphate (PI(3,4,5)$P_3$ or $PIP_3$) accumulation in membranes is essential for the recruitment of Akt to membrane compartments for subsequent mTORC2- and PDK1-induced activation of Akt via phosphorylation of Akt at Ser$^{473}$ and Thr$^{308}$, respectively (Alessi et al., 1996, Manning and Toker, 2017). As PINK1 enhances Akt phosphorylation at both Ser$^{473}$ and Thr$^{308}$ sites, we hypothesised that PINK1 may regulate PI3-kinase and PTEN, the primary enzymes that control the synthesis and degradation of $PIP_3$, respectively (Hers et al., 2011). The levels of the PI3-kinase catalytic subunit, pl10α, were not altered by PINK1 expression (Fig. 4B). However, activation of the regulatory subunit PI3-kinase p85 (as measured by the phospho-p85 (pTyr458) (Aweida et al., 2018, Ibrahim et al., 2019, Pedrosa et al., 2019, Zheng et al., 2019) /p85α ratio) was significantly decreased by PINK1 deletion. This p85 activation was restored in hPINK1$_{res}$, but not in hPINK1$_{TKD}$ (Fig. 4B). In contrast, neither total PTEN levels, nor its phosphorylation at Ser$^{380}$

(inactivating residue), were significantly altered by PINK1 knockout or overexpression (Fig. 4C). Together these data indicate that activation of Akt by PINK1 may be mechanistically linked to PI3-kinase phosphorylation, specifically the p85 regulatory subunit.

**PINK1 kinase activity regulates the dynamic subcellular localisation of $PIP_3$ at the plasma membrane and Golgi in response to IGF-1.**

Initial rapid plasma membrane and subsequent longer-term endomembrane localisation of $PIP_3$, particularly in the Golgi and ER, in response to agonists / growth factors are critical determinants of compartment-specific Akt activation (Ebner et al., 2017, Jethwa et al., 2015, Manning and Toker, 2017, Sato et al., 2003). We employed a $PIP_3$-specific monoclonal antibody (Braccini et al., 2015, Moult et al., 2010, Papakonstanti et al., 2007, Wang et al., 2010) to determine whether PINK1 modulated the subcellular localisation of $PIP_3$ under normal growth conditions and in response to short- (2, 10 min) and longer-term (60 min) IGF-1 stimulation. Following 24 h serum deprivation, $PIP_3$ was diffusely distributed throughout all cells (Fig. 5A). Non-uniform accumulations of $PIP_3$ at the plasma membrane in response to IGF-1 were evident in $hPINK1_{res}$ after 2 min, but not in $PINK1^{+/+}$, $PINK1^{-/-}$, or $PINK1_{TKD}$ MEFs (Fig. 5A). After 10 min of IGF-1 stimulation, $PIP_3$ was observed at specific plasma membrane domains in all four cell lines (Fig. 5A). Importantly, PI3-kinase inhibition, by pretreatment with LY294002 (10 μM), prevented production of $PIP_3$ at the plasma membrane in all three cell types. However, $hPINK1_{res}$-expressing cells had distinctly increased $PIP_3$ levels near the plasma membrane, in the presence of LY294002 10 μM (Fig. 5A) and also using increased concentrations of LY294002 50 μM (data not shown).

We observed that $PIP_3$ localises predominantly in the perinuclear region during normal growth conditions (Fig 5B) compared to its localisation in distinctive loci at the plasma membrane following 10-min stimulation with IGF-1 (Fig. 5A). To determine the subcellular localisation of $PIP_3$ in this perinuclear region, we performed double immunofluorescence co-localisation analysis of $PIP_3$ with a number of selective endomembrane markers (Rab14: early endosomes, Rab11a: recycling endosomes, GRP-78-BIP: endoplasmic reticulum, Giantin: medial-Golgi, TGN46: trans-Golgi and Lysotracker: lysosomes) (Supp. 3). We further sought to determine whether PINK1 deletion modified the localisation of $PIP_3$ within any specific endomembrane compartment. The results revealed a selective localisation of

$PIP_3$ to the medial-Golgi, as the medial-Golgi protein, Giantin, displayed the greatest colocalisation with $PIP_3$ (42.9% in $PINK1^{+/+}$ and 48.3% $hPINK1_{res}$ cells) (Fig. 5B). Notably, there was a significant reduction in the colocalisation of $PIP_3$ and Giantin in $PINK1^{-/-}$ and $hPINK1_{TKD}$ MEFs (16.9% and 17.8%, respectively, $p < 0.0001$) (Fig. 5B). Furthermore the colocalisaton of $PIP_3$ within the medial-Golgi was selective, since $PIP_3$ colocalisation with the trans-Golgi marker, TGN46, and all other endomembrane markers was significantly lower than that measured for Giantin (15-20%) and moreover was not altered by PINK1 deletion or PINK1 kinase activity (Supp. 3). The only exception to this was a significant reduction of $PIP_3$ colocalisation with Rab14 in $PINK1^{-/-}$ cells ($p < 0.0005$) compared to wild-type MEFs, although the colocalisation of $PIP_3$ was rather low in these cells (27%). Moreover, the reduced colocalisation of $PIP_3$ with Rab 14 was only partially rescued by overexpression of PINK1 and was not PINK1 kinase-dependent (Supp. 3).

Interestingly a time lag for $PIP_3$ localisation to the Golgi after PDGF, EGF and insulin stimulation has been described (Ebner et al., 2017). We sought to determine if this was also apparent in response to IGF-1 and furthermore whether this was regulated by PINK1. Our results show that following short-term IGF-1 stimulation (10 min) the colocalisation of $PIP_3$ with Giantin was low in all cell lines ($PINK1^{+/+}$ 17.6%, $PINK1^{-/-}$ 10%, $hPINK1_{res}$ 15.7%, $hPINK1_{TKD}$ 17.4%) (Fig. 5C). However, longer-term stimulation with IGF-1 (60 min) resulted in a moderate increase in the colocalisation of $PIP_3$ with Giantin in wildtype and $hPINK1_{res}$ cells (26% and 20% respectively), but not in $PINK1^{-/-}$ and $hPINK1_{TKD}$ MEFs (13.9% and 11.5% respectively) (Fig. 5C). Together, these results indicate that $PIP_3$ localises to the medial-Golgi under normal growth conditions, and that PINK1 kinase activity plays a key role in regulating the localisation of $PIP_3$ to the medial-Golgi.

**PINK1 colocalises with $PIP_3$ and protects against Golgi fragmentation with Akt dependency**

PINK1 has been reported to have a dynamic subcellular localisation including within the cytosol (Dagda et al., 2009, Dagda et al., 2014, Dickey and Strack, 2011, Fedorowicz et al., 2014, Ries et al., 2006, Steer et al., 2015, Xiong et al., 2009), with increased localisation of PINK1 at the mitochondria when mitochondria are depolarised (Kane et al., 2014, Kazlauskaite et al., 2014, Kondapalli et al., 2012, Koyano et al., 2014, Matsuda et al., 2010, Shiba-Fukushima et al., 2012, Vincow et al., 2013, Ziviani et al., 2010). Due to our discovery

that PINK1 could modulate $PIP_3$ localisation both at the plasma membrane and the medial-Golgi in a PINK1-kinase dependent fashion, we investigated the possible colocalisation of overexpressed His-tagged $hPINK1_{res}$ and $PIP_3$. Our results reveal a clear colocalisation of His-tagged $hPINK1_{res}$ and $PIP_3$ (Fig. 6A).

Golgi fragmentation is a known characteristic of PD neuropathology (Fujita et al., 2006, Gosavi et al., 2002, Rendon et al., 2013). Because of our findings that PINK1 could colocalise with $PIP_3$ and regulate levels of $PIP_3$ in the medial-Golgi, we were interested to determine if PINK1 regulated Golgi morphology. We employed both Giantin and GM130 to examine Golgi morphology and we found that $PINK1^{-/-}$ MEFs demonstrated significant levels of Golgi fragmentation during serum deprivation (Fig. 6B). Notably, Golgi fragmentation was rescued by hPINK1 overexpression and was PINK1 kinase-dependent (Fig. 6B). We further showed that this aberrant Golgi morphology was not altered by short- (10 min) or long-term (60 min) stimulation with IGF-1 in the absence of PINK1 kinase activity. We next hypothesised that increased PINK1 kinase-induced localisation of $PIP_3$ in the medial-Golgi protected against Golgi fragmentation via Akt activation. To investigate this, we treated $hPINK1_{res}$ MEFs with the selective Akt inhibitor MK2206 (Yap et al., 2011). Low concentrations (1 μM) of MK2206 prevented Akt activation with no significant effect on cell survival in hPINK1res MEFs (Fig. 6C). Furthermore, PINK1-induced protection from Golgi fragmentation, evident in hPINK1res MEFs, was completely blocked by Akt inhibition (Fig. 6D). Together, these results indicate that PINK1 kinase activity promotes Akt activity, that it dynamically regulates its major activating lipid $PIP_3$, particularly at the medial-Golgi, and that PINK1 kinase-dependent Akt activation protects against Golgi fragmentation.

**PINK1 can modulate the cellular levels of $PIP_3$ and $PIP_2$**

Finally, we were interested to determine whether PINK1 could directly regulate total cellular phosphatidylinositol (PI) levels. Using advanced mass-spectrometry approaches (Kielkowska et al., 2014) we measured total levels of phosphatidylinositol (PI), phosphatidylinositol phosphate (PIP), $PIP_2$ and $PIP_3$ in wild type and PINK1-modified MEFs under normal growth conditions, following 24 h serum deprivation and upon 10-min IGF-1 stimulation. $PIP_3$ levels were significantly reduced in $PINK1^{-/-}$ MEFs in normal growth medium (but not in serum deprivation conditions or in response to IGF-1 stimulation); this was partially rescued by $hPINK1_{res}$ but was not kinase-dependent (Supp. 4B). $PIP_2$ levels were significantly lower in

PINK1$^{-/-}$ cells in response to IGF-1 stimulation (but not in normal growth medium or under serum deprivation conditions) and this was partially rescued by hPINK1$_{res}$ but was not kinase-dependent (Supp. 4C). There were no significant differences in levels of PI and PIP between PINK1$^{+/+}$, PINK1$^{-/-}$, hPINK1$_{res}$ and hPINK1$_{TKD}$ cells (Supp. 4D, E). Thus PINK1 kinase activity can selectively modulate the total cellular levels of $PIP_2$ and $PIP_3$, under certain conditions. However, this does not appear to directly underpin the regulation of normal and IGF-1-induced subcellular localisation of $PIP_3$ by PINK1 kinase activity.

## Discussion

The serine threonine kinase PINK1 has been extensively investigated since its discovery as an autosomal recessive PD-causing gene (Valente et al., 2004). PINK1 activates and interacts with PI3-kinase/Akt signalling to induce cell survival, mitochondrial integrity and stress resistance (Akundi et al., 2012, Boonying et al., 2019, Contreras-Zarate et al., 2015, Ellis et al., 2013, Hauser et al., 2017, Maj et al., 2010, Mei et al., 2009, Murata et al., 2011, O'Flanagan et al., 2015, O'Flanagan and O'Neill, 2014, Sanchez-Mora et al., 2012, Soutar et al., 2018). Notably, Akt activity is significantly reduced in both in vitro PD models and human dopaminergic PD substantia nigral neurons (Malagelada et al., 2008, Timmons et al., 2009). However, the mechanisms by which Akt activation becomes impaired due to loss of PINK1 function in PD are unclear. In this study, we show that PINK1 is a primary upstream activator of Akt during normal growth, and constitutively activates Akt in the absence of growth factors. We reveal for the first time that promotion of Akt activation by PINK1 is PINK1 kinase-dependent, and that PINK1 kinase activity enhances Akt recruitment to the plasma membrane during normal growth and in response to IGF-1. We show that PINK1 regulates the phosphorylation of PI3-kinase p85, colocalises with its product $PIP_3$, the lipid essential for Akt membrane recruitment, vital for Akt activation (Manning and Toker, 2017). Furthermore, we show that PINK1 dynamically increases $PIP_3$ levels at the plasma membrane and Golgi in response to short- and longer-term IGF-1 stimulation, respectively, and during normal growth. We demonstrate that PINK deletion induces Golgi fragmentation, a known characteristic of PD neuropathology. Importantly, we show that PINK1 overexpression restores normal Golgi morphology and that this depends on activation of PINK1 kinase and

of Akt. Together these data provide novel insights into mechanisms by which loss of PINK1 function causes Akt signalling defects in PD.

Full Akt activation requires mTORC2-induced phosphorylation of Akt at $Ser^{473}$ in the C-terminal hydrophobic motif (Alessi et al., 1996, Sarbassov et al., 2005, Stokoe et al., 1997) and PDK-1 phosphorylation of Akt at $Thr^{308}$ in the activation loop (Calleja et al., 2007, Stokoe et al., 1997), for review (Manning and Toker, 2017). MEFs derived from $PINK1^{-/-}$ mice display impaired IGF-1-dependent Akt phosphorylation at both $Ser^{473}$/$Thr^{308}$ activating residues (Akundi et al., 2012). The present study is the first to reveal that phosphorylation at both Akt-activating residues in $PINK1^{-/-}$ MEFs can be rescued by PINK1 overexpression and is PINK1 kinase-dependent. Our results further indicate that the impact of PINK1 appears to be more prominent for phosphorylation at $Ser^{473}$ than $Thr^{308}$. Notably, the activation of Akt is extremely diminished in the absence of $Ser^{473}$ phosphorylation (Alessi et al., 1996, Yang et al., 2002). One recent study concluded that $PIP_3$ activation of Akt is predominantly due to recruitment of Akt to $PIP_3$ in membranes to facilitate PDK1 and mTORC2 catalysed Akt phosphorylation (Chu et al., 2018). However in contrast, another recent study found that $PIP_3$ binding allosterically activates Akt and that dissociation from $PIP_3$ is rate limiting for Akt dephosphorylation (Ebner et al., 2017). It is thus possible that our results indicate that PINK1 inhibits $PIP_3$ dissociation that favours Akt phosphorylation at $Ser^{473}$ over $Thr^{308}$ by more effectively blocking $Ser^{473}$ dephosphorylation. The more pronounced effect of PINK1 on $Ser^{473}$ phosphorylation may be further due to regulation of a number of properties reported for $Ser^{473}$ phosphorylation (Chu et al., 2018, Lucic et al., 2018, Manning and Toker, 2017) or possible regulation by mTORC2 (Murata et al., 2011).

Furthermore, our results demonstrate that PINK1 can constitutively activate Akt, increasing phosphorylation at both activating residues, even in the absence of growth factors, and that this is dependent on PINK1 kinase activity. This places PINK1 kinase as a primary upstream activator of Akt, in agreement with studies which showed that PINK1 is necessary for maximal responses of Akt to growth factors (Akundi et al., 2012, Contreras-Zarate et al., 2015, Ellis et al., 2013, Maj et al., 2010, Manning and Toker, 2017, Mei et al., 2009, Murata et al., 2011, Sanchez-Mora et al., 2012), preventing apoptosis, promoting cell survival and protecting against several cell stressors (Akundi et al., 2012, Contreras-Zarate et al., 2015, Murata et al., 2011, Sanchez-Mora et al., 2012). Importantly, it has been shown that PINK1 mRNA expression is induced by FOXO3a, a major stress-resistant transcription factor, which is up-regulated in the absence of Akt activation when growth factors and nutrients are absent

(Mei et al., 2009). Our results showing that PINK1 can activate Akt constitutively when growth factors and nutrients are absent may indicate a role for this pathway in the short-term protection necessary to sustain cells until growth factors are available. The PI3-kinase/Akt pathway is intimately linked with mitochondrial respiration, prevention of mitochondrial apoptosis, and metabolic rewiring via enhanced glycolysis, including in cancer cells for review (O'Flanagan and O'Neill, 2014). ). PINK1 has been most studied as a key regulator of mitochondrial health, particularly in the regulation of mitophagy via the PINK1/parkin mitophagy pathway (Harper et al., 2018, Kane et al., 2014, Kawajiri et al., 2010, Kazlauskaite et al., 2014, Kondapalli et al., 2012, Koyano et al., 2014, Matsuda et al., 2010, Pilsl and Winklhofer, 2012, Soutar et al., 2018, Vincow et al., 2013, Youle and Narendra, 2011, Youle and van der Bliek, 2012). Previous studies showed that inhibition of Akt with MK2206 blocks the PINK1/parkin pathway (Hauser et al., 2017, McCoy et al., 2014). More recent studies show that Akt signalling regulates PINK1-dependent mitophagy (Soutar et al., 2018). In these contexts, Akt activation was placed upstream of PINK1 and it was recognised that the reciprocal regulation of PINK1 by Akt and Akt by PINKI is important in mitophagy regulation (Soutar et al., 2018).

Our major aim was to determine the mechanism by which PINK1 promotes Akt activation. We hypothesised that PINK1 may induce both PDK-1 phosphorylation of Akt at $Thr^{308}$ and mTORC2-induced phosphorylation of Akt at $Ser^{473}$ (Alessi et al., 1996, Sarbassov et al., 2005, Stokoe et al., 1997). Interestingly, previous studies showed that PINK1 can induce mTORC2 activation of $Ser^{473}$ in the absence of $Thr^{308}$ phosphorylation. This was indicated to be via Rictor, and to occur independently of PI3-kinase (Murata et al., 2011). In contrast, we found that PINK1-induced increased phosphorylation of Akt at both $Ser^{473}$ and $Thr^{308}$ residues was not associated with altered levels of active PDK1 or of Rictor. The discrepancies between these studies regarding the mechanisms by which PINK1 can activate Akt may be due to cell- or agonist-specific effects.

Dynamic, rapid, and transient agonist-induced accumulation of Akt at the plasma membrane is essential for growth factor- and agonist-induced Akt activation (Manning and Toker, 2017) for review, and can be monitored by GFP-Akt-PH transfection (Calleja et al., 2007, Ebner et al., 2017, Meyer et al., 2012). Our results provide novel data showing that PINK1 significantly accelerates this recruitment of GFP-Akt-PH and GFP-Akt to the plasma membrane with PINK1 kinase-dependency, both in normal growth media and in response to shorter-term IGF-1 stimulation. The recruitment of Akt to the plasma membrane occurs via

its PH domain and relies predominantly on increased, localised and rapid production of $PIP_3$ (Calleja et al., 2007, Manning and Toker, 2017). These initial rapid plasma membrane and subsequent longer-term endomembrane localisations of $PIP_3$, particularly in the Golgi and ER, in response to agonists / growth factors are critical determinants of compartment-specific Akt activation (Ebner et al., 2017, Jethwa et al., 2015, Manning and Toker, 2017, Sato et al., 2003). These results drew us to explore the possibility that PINK1 may regulate the production of $PIP_3$ within the plasma membrane and endomembranes. We show that PINK1 kinase activity accelerates the production of $PIP_3$ towards the plasma membrane in response to short-term stimulation by IGF-1 (2 and 10 min). Interestingly, several cells expressing $hPINK1_{res}$ had distinct areas of $PIP_3$ immunoreactivity near the plasma membrane, even in the presence of the PI3-kinase inhibitor. There may be both PI3-kinase dependent and independent mechanisms responsible for the PINK1-induced $PIP_3$ increases. The changes in PI3-kinase phosphorylation indicate that activation of Akt by PINK1 may be mechanistically linked to the p85 regulatory subunit. However, p85α/β has many functions that do not involve PI3-kinase activation, for example, p85α can regulate PTEN (Chagpar et al., 2010, Cheung et al., 2015, Rabinovsky et al., 2009) and the PI3-kinase p110α subunit catalytic activity can occur independent of p85α/β (Thorpe et al., 2017, Tsolakos et al., 2018).

We further show that His-tagged PINK1 displays a very strong co-localisation with $PIP_3$, throughout the cell during normal growth, further supporting PINK1's function as a regulator of $PIP_3$ within both plasma- and endo-membranes. A previous study using spatio-temporal examination of $PIP_3$ production in living cells, following ligand stimulation, demonstrated that $PIP_3$ levels increase to a larger extent in endomembranes (ER and Golgi) than at the plasma membrane (Sato et al., 2003). In agreement, we show that $PIP_3$ is predominantly localised in the perinuclear region during normal growth. We performed a detailed analysis to determine the endomembrane localisation of $PIP_3$ and demonstrate a strong selective co-localisation of $PIP_3$ with Giantin in the medial-Golgi compartment. Importantly, we further show that PINK1 deletion significantly and selectively reduces the localisation of $PIP_3$ to the medial-Golgi, during normal growth, and moderately in response to longer-term IGF-1 stimulation (60 min), and show that this is PINK1 kinase-dependent. In agreement with our study, a time-lag for $PIP_3$ localisation to the Golgi has been shown following PDGF, EGF and insulin stimulation of Akt in HeLa and MCF-7 cells (Ebner et al., 2017). The Golgi plays a pivotal role in the compartmentalisation of cell signalling initiating at the plasma membrane (Peng et al., 2014). Our results thus indicate a new role for PINK1 kinase activity in the

regulation of $PIP_3$ responses in the plasma membrane, Golgi and endomembranes, which are known to be important for both compartmentalised and temporal regulation of Akt substrate phosphorylation (Ebner et al., 2017, Jethwa et al., 2015, Manning and Toker, 2017, Sato et al., 2003). Furthermore, $PIP_3$ generation *in situ*, primarily in the Golgi and ER, has been shown to depend on endocytosis of activating receptor tyrosine kinases. Interestingly, in this respect it has been reported that PINK1 deficiency disturbs the intracellular localisation of the IGF-1 receptor (Contreras-Zarate et al., 2015).

Although we did not detect Akt in the Golgi network we do think there is potential it is also present here. The main tools employed were GFP-Akt and GFP-Akt-PH constructs, and we do not see any Golgi localisation with either of these. However, these constructs may favour the plasma membrane and the concentration of Akt may be higher at the plasma membrane than in endomembrane compartments in these PINK1 modified MEFs. Thus, the availability of more sensitive tools such as improved Akt antibodies may uncover Akt in the Golgi, and the endosomal-ER-Golgi network.

In healthy cells, the Golgi apparatus is a ribbon-like structure made up of flattened, parallel cisternae which are interconnected in the perinuclear region (Nakagomi et al., 2008), as we observe in wild type MEFs. Numerous studies have shown that during cell stress or apoptotic cell death, Golgi stacks disassemble into tubulovesicular clusters, a process known as fragmentation of the Golgi apparatus (Alvarez-Miranda et al., 2015, Chiu et al., 2002, Fan et al., 2008, Lane et al., 2002, Machamer, 2003). Golgi fragmentation has been reported in nigral neurons in postmortem samples of PD brain (Fujita et al., 2006) and in in vitro PD models (Gosavi et al., 2002, Rendon et al., 2013). Furthermore, bioinformatics modelling has linked stress-induced Golgi fragmentation to a number of neurodegenerative processes (Alvarez-Miranda et al., 2015). We reveal for the first time that PINK1 deletion causes significant Golgi fragmentation, and importantly, we show that this is prevented by PINK1 overexpression and dependent on PINK1 kinase activity. This is a significant new function for PINK1 and furthermore is linked mechanistically to impaired Akt signalling caused by PINK1 deletion. Thus, we show that Akt inhibition in cells overexpressing PINK1 prevents the ability of PINK1 to protect against Golgi fragmentation. Interestingly, inhibition of $PI(4,5)P_2$ synthesis in GH3 cells has been reported to lead to Golgi fragmentation, linking phosphoinositides with the structural integrity of the Golgi apparatus (Siddhanta et al., 2003).

In this study, we demonstrate that impaired activation of Akt, via loss of PINK1 kinase function, as occurs in PD, centers on defects in $PIP_3$ regulation upstream of Akt activation. Our mass spectrometry analysis showed that total levels of $PIP_3$ and $PIP_2$, but not PIP and PI, lipids were modulated by PINK1 deletion in some contexts, but not regulated in a PINK1 kinase-dependent manner. This infers that PINK1 kinase regulates selective membrane pools of $PIP_3$ rather than total $PIP_3$ levels. It is important to note that several risk genes for PD regulate the PI3-kinase/Akt signalling axis, including *Parkin* (Fallon et al., 2006, Gupta et al., 2017), *DJ-1* (Jaramillo-Gomez et al., 2015, Kim et al., 2011, Zhang et al., 2016), *LRKK2* (Chuang et al., 2014, Ohta et al., 2011) and *SNCA* (Seo et al., 2002). Importantly, defects in Akt signalling occur in nigral neurons in the PD brain (Malagelada et al., 2008, Timmons et al., 2009), drawing attention to the relevance of targeting this vital survival and metabolic system for neuroprotection in PD. Phosphoinositide-protein interactions are at the hub of both Akt and other major signalling axes and play integral roles in vesicular trafficking. These are key systems known to be regulated by PD risk genes (Cao et al., 2017, Krebs et al., 2013, Vanhauwaert et al., 2017) and to become impaired in PD (Kutateladze, 2010, Wenk and De Camilli, 2004). Our study provides new mechanistic insights for a modulation of the core $PIP_3$-Akt regulatory machinery by PINK1 kinase activity, presenting a novel mechanism that may underlie impaired activation of the vital Akt signalling machinery in PD. This draws attention to the integration of phosphoinositide and protein networks in the understanding and therapeutic targeting of key systems, including Akt, that become defective in the neurodegenerative processes underlying PD.

## Materials and Methods

### Generation of PINK1$^{-/-}$ mice and derived MEF cell lines

The cell lines used in these experiments are Mouse Embryonic Fibroblast (MEF) cells, as previously employed and described (Glasl et al., 2012, Morais et al., 2009, O'Flanagan et al., 2015). PINK1$^{-/-}$ knockout and PINK1$^{+/-}$ heterozygous knockout mice were generated by Wolfgang Wurst and Daniela Vogt-Weisenhorn (Helmholtz Center, Munich, Germany) and immortalised MEFs were generated as previously described (Morais et al., 2009). In brief, PINK1$^{+/-}$ mice were interbred to generate mutant mice and wild-type littermate controls. Embryonic day 13 mice were dissected, heads and red organs removed and used for

genotyping. The rest of the bodies were chopped up in cell culture dishes containing Dulbecco's modified Eagle's medium supplied with 50% fetal bovine serum and 1% penicillin/streptomycin. Cultures were expanded and serum decreased to 10% fetal bovine serum after the attainment of consistent growth. Afterward cultures were immortalised by transfection with simian virus 40 (SV40) large T-antigen. PINK1$^{-/-}$ MEFs were stably transfected with a plasmid containing human PINK1 (hPINK1 construct Origene (Rockville, MD, USA)), and the triple kinase dead hPINK1$_{K219A/D362A/D384A}$ mutants using site-directed mutagenesis (Stratagene, Santa Clara, CA, USA). The triple kinase dead mutation for PINK1 is not known to affect the stability/conformation of the PINK1 (Pridgeon et al., 2007). Cells were routinely monitored for mycoplasma and bacterial/yeast contaminations.

**RT-PCR**

PINK1 deletion/expression was confirmed in MEF cell lines employed in this study using RNA extraction and RT-PCR analysis (Supp. 4A). RNA was extracted using the PureLink RNA Mini Kit (Thermo Scientific) according to the instructions of the manufacturer. cDNA synthesis was performed with the QuantiTect reverse transcription kit (Qiagen) using 1µg of RNA. The primers and conditions used for RT-PCR are shown in supplementary information, this was performed using the GoTaq G2 Green Master Mix kit (Promega).

**Cell Culture and stimulation/inhibition of the PI3-kinase/Akt pathway**

MEFs were cultured in Dulbecco's Modified Eagle Medium: High glucose (DMEM-Hi), supplemented with 10% fetal bovine serum (FBS) and 2 mM L-Glutamine. Cells were cultured at 37$^0$C in a humidified incubator supplemented with 5% $CO_2$. In IGF-1 stimulation experiments, cells were plated overnight with complete media, followed by incubation with serum-free DMEM-Hi for 24 h. After 24 h, 10 ng/ml IGF-1 was added at the specified time-points (2, 10 or 60 min). In experiments for inhibition of PI3-kinase, cells were plated overnight with complete media, incubated with serum-free DMEM-Hi for 24 h, followed by incubation with 10 µM LY294002 for 30 min and subsequent stimulation with 10 ng/ml IGF-1 for 10 min. In experiments for MK2206 inhibition, cells were plated overnight with complete media, serum deprived for 24 h and then incubated with 1µM for MK2206 for 1 or 4 h. For Lysotracker and $PIP_3$ colocalisation analysis (Fig. 3), 75 nM of Lysotracker was added to the cells in culture for 1 h before fixation with 3% PFA for immunocytochemistry. BE(2)-M17 cells, transduced with PINK1 shRNA (PINK1A8, PINK1C2) or with control

shRNA (Control 1, Control 2), were kindly provided by Mark Cookson and Alexandra Beilina NIA, Bethesda, MD, USA and were transduced and cultured as previously described (Sandebring et al., 2009).

**Plasmids**

The GFP-Akt-PH construct was kindly provided by Martin Lowe (University of Manchester, Manchester, UK). pEGFP-Akt was a gift from Julian Downward (Addgene plasmid # 39531; http://n2t.net/addgene:39531 ; RRID:Addgene_39531) (Watton and Downward, 1999). MEFs were seeded in 24-well plates to be 70% confluent the following day. Cells were then transfected with GFP-Akt-PH or GFP-Akt using Lipofectamine™ as recommended by the manufacturer's instructions.

**Western Immunoblotting**

The following primary antibodies, dilutions and sources were used: Akt (1:1,000) (Cell Signalling #9272), Akt 1 (1:1,000) (Cell Signalling #2938), Akt 2 (1:1,000) (Cell Signalling #3063), Akt 3 (1:1,000) (Cell Signalling #8018), P-Akt pSer$^{437}$ (1:500) (Cell Signalling #4060), P-Akt pThr$^{308}$ (1:500) (Cell Signalling #9275), P-PDK1$^{Ser241}$ (1:500) (Cell Signalling #3061), P-PI3-kinase p85$^{Tyr458}$/p55$^{Tyr199}$ (1:500) (Cell Signalling #4228), PI3-kinase p85α (1:1,000) (Cell Signalling #4257), PI3-kinase p110α (1:500) (BD Transduction Laboratories 611399), PTEN (1:500) (Cell Signalling #9552), P-PTEN$^{Ser380}$ (1:500) (Cell Signalling #9551), RICTOR (1:500) (Cell Signalling #2114), β-actin (1:16,000) (Sigma Aldrich A5441). Primary antibodies were detected using horseradish peroxidase (HRP)-conjugated isotype-specific anti-rabbit IgG or anti-mouse IgG (1:1000, DAKO, Cambridgeshire, UK) secondary antibodies.

Western immunoblotting was carried out as described previously (Griffin et al., 2005, Moloney et al., 2010, O'Flanagan et al., 2015). Briefly, proteins were extracted, separated by SDS-PAGE (20μg/lane) and transferred electrophoretically to nitrocellulose membranes using a wet transfer apparatus and transfer buffer consisting of 48 mM Tris base, 39 mM glycine and 20% ethanol. After blocking for 1 h in 5% milk or 30 min in 5% Bovine Serum Albumin (phospho antibodies), cells were incubated in primary antibody solutions overnight at 4ºC. The blot underwent three 10-min washes in 1X TBX-T prior to secondary antibody incubation. Cells were incubated in secondary antibody solution for 1 h at RT followed by three 5-min washes in 1X TBS-T. Immunoreactive proteins were detected with enhanced

chemiluminescence (Amersham Biosciences, Little Chalfont, UK). All quantifications are illustrated by histograms which represent the densitometry of each protein normalised to β-Actin for an n = 3 as determined by ImageJ software.

**Immunofluorescence and confocal microscopy**

The following primary antibodies and dilutions were used: Phosphatidylinositol (3,4,5)-trisphosphate (1:150) (Tebu-Bio 117Z-P345B), Giantin (1:300) (kindly provided by Martin Lowe, University of Manchester), GM130 (1:4,000) (BD biosciences 610822), GRP-78-BIP (1:800) (Abcam Ab21685), His (1:400) (Abcam #9108) Rab 11a (1:100) (Zymed 715300), Rab14 (1:500) (Sigma R0656) and TGN46 (1:500) (Serotek UK AHP500). Primary antibodies were detected using Cy3 anti-rabbit IgG (1:400) (Jackson laboratories 711-165-152) or Alexa Fluor 488 conjugated anti-mouse IgG (1:400) (Invitrogen A11001) secondary antibodies.

Culture medium was removed from each of the wells. Cells were washed with 1X PBS in-between each of the following steps: fixation in 0.5 ml 3% paraformaldehyde (PFA) for 15 min at room temperature, quenching in 1 ml of 50 mM $NH_4Cl$/PBS for 15 min, permeabilisation in 1 ml buffer (0.05% Saponin/PBS, 0.2% BSA/PBS) for 5 min. Coverslips were transferred to a humid box and primary antibodies were added at appropriate dilutions in 5% BSA/PBS. Primary antibodies were incubated for 2 h at room temperature. Then cells were washed twice in 1X PBS. Cells were incubated in secondary antibody solutions in 5% BSA/PBS, as well as DAPI/PBS (1:10,000) for 1 h at room temperature. Cells were washed twice with 1X PBS for 5 min. Coverslips were mounted onto microscope slides using Mowiol mounting media. Cells were dried overnight and fluorescence images were acquired using Zeiss LSM 510 Meta confocal microscope fitted with a 63x/1.4 plan apochromat lens (Jena, Germany).

For GFP-Akt-PH analysis, each experiment was performed in duplicate. For the two coverslips per condition > 200 cells were counted. The threshold of intensity used was fluorescence in the cytosol as the baseline and any fluorescence intensity level above that at the plasma membrane (PM) was judged as an accumulation at the PM. To quantify the localisation of Akt at the PM the total number of transfected cells and the number of cells with Akt at the plasma membrane were counted (determined as described above). From these

values the percentage of cells with Akt at the PM was then calculated for n = 3 and the representative histogram generated in GraphPad. To determine fluorescence intensity at the plasma membrane a line plot was drawn through the cell using the plot profile analysis in Carl Zeiss Zen 2.1 image analysis software, as described previously (Lindsay and McCaffrey, 2009). The X-axis represents distance along the line and the Y-axis is the pixel intensity. Pearson's colocalisation coefficient was calculated using Zeiss ZEN 2009 software as described previously (Lindsay et al., 2013).

**Mass spectrometry**

Mass spectrometry was used to measure inositol lipid levels essentially as previously described (Clark et al., 2011), using a QTRAP 4000 (AB Sciex) mass spectrometer and employing the lipid extraction and derivitisation method described for cultured cells, with the modification that 10 ng C17:0/C16:0 PtdIns(3,4,5)$P_3$ internal standard (ISD) and 10 ng C17:0/C16:0 PtdIns ISD were added to primary extracts, and that final samples were dried in a Speedvac concentrator rather than under liquid $N_2$. Measurements were conducted in duplicate for three separate experiments, on $3x10^5$ cells per sample. PIP, $PIP_2$ and $PIP_3$ response ratios were calculated by dividing PIP, $PIP_2$ and $PIP_3$ response areas by the corresponding response areas of $PIP_2$ (for PIP and $PIP_2$) and $PIP_3$ ($PIP_3$ only) ISD in each sample. PIP, $PIP_2$, and $PIP_3$ responses were normalised to PI response ratio to account for any cell input variability.

**Crystal Violet staining**

Crystal violet staining was used for assaying cell survival in response to treatment with MK2206. Cells were fixed with 4% PFA for 20 min, followed by staining with 0.05% crystal violet in 20% ethanol for 30 min. Cells were washed with $dH_20$ and let to dry overnight and images were acquired using the Odyssey imaging system.

**Statistical analysis**

All data were analysed using GraphPad Prism. Data are expressed as means ± the standard error of the mean (SEM). Statistical analysis was carried out using one-way ANOVA, followed by a post-hoc Tukey test if the ANOVA indicated significance. Differences were considered significant at $p < 0.05$.

**Acknowledgments**

We are thankful to Bart De Strooper VIB Center for the Biology of Disease, VIB, Leuven, Belgium and Center for Human Genetics and LIND, K.U. Leuven, Leuven, Belgium and Vanessa Morais Instituto de Medicina Molecular Lisboa, Portugal, for providing us with PINK1 modified Mouse Embryonic Fibroblast cells. We are grateful to Mark Cookson and Alexandra Beilina, National Institute on Aging, Bethesda, MD, USA for providing us with BE(2)-M17 cells transduced with control and PINK1 shRNA. This work was funded by the Irish Research Council Government of Ireland Postgraduate Scholarship Programme. The Molecular Cell Biology group, UCC, provided access to a Zeiss 510 Confocal microscope, funded by an SFI Programme Grant to Mary W. McCaffrey.

**Author contributions**

Rachel Furlong: study conception, investigation, performed experiments, data and evidence collection, formal analysis, and manuscript preparation.

Andrew Lindsay: manuscript preparation, commentary, critical review.

Karen E. Andersson: mass spectrometry for phosphoinositide analysis, commentary, critical review

Phillip T. Hawkins: mass spectrometry for phosphoinositide analysis, commentary, critical review

Aideen Sullivan: study conception, supervision, manuscript preparation, commentary, critical review.

Cora O Neill: study conception, supervision, manuscript preparation, commentary, critical review.

**Conflict of Interest**

The authors declare no conflict of interest.

## References


AKUNDI, R. S., ZHI, L. & BUELER, H. 2012. PINK1 enhances insulin-like growth factor-1-dependent Akt signaling and protection against apoptosis. *Neurobiol Dis,* 45**,** 469-78.

ALESSI, D. R., ANDJELKOVIC, M., CAUDWELL, B., CRON, P., MORRICE, N., COHEN, P. & HEMMINGS, B. A. 1996. Mechanism of activation of protein kinase B by insulin and IGF-1. *Embo j,* 15**,** 6541-51.

ALVAREZ-MIRANDA, E. A., SINNL, M. & FARHAN, H. 2015. Alteration of Golgi Structure by Stress: A Link to Neurodegeneration? *Front Neurosci,* 9**,** 435.

ARENA, G., GELMETTI, V., TOROSANTUCCI, L., VIGNONE, D., LAMORTE, G., DE ROSA, P., CILIA, E., JONAS, E. A. & VALENTE, E. M. 2013. PINK1 protects against cell death induced by mitochondrial depolarization, by phosphorylating Bcl-xL and impairing its pro-apoptotic cleavage. *Cell Death Differ,* 20**,** 920-30.

ARENA, G. & VALENTE, E. M. 2017. PINK1 in the limelight: multiple functions of an eclectic protein in human health and disease. *J Pathol,* 241**,** 251-263.

AWEIDA, D., RUDESKY, I., VOLODIN, A., SHIMKO, E. & COHEN, S. 2018. GSK3-beta promotes calpain-1-mediated desmin filament depolymerization and myofibril loss in atrophy. *J Cell Biol,* 217**,** 3698-3714.

BELLACOSA, A., CHAN, T. O., AHMED, N. N., DATTA, K., MALSTROM, S., STOKOE, D., MCCORMICK, F., FENG, J. & TSICHLIS, P. 1998. Akt activation by growth factors is a multiple-step process: the role of the PH domain. *Oncogene,* 17**,** 313-25.

BOONYING, W., JOSELIN, A., HUANG, E., QU, D., SAFARPOUR, F., IYIRHIARO, G. O., RODRIGUEZ GONZALEZ, Y., CALLAGHAN, S. M., SLACK, R. S., FIGEYS, D., CHUNG, Y. H. & PARK, D. S. 2019. Pink1 regulates FKBP5 interaction with AKT/PHLPP and protects neurons from neurotoxin stress induced by MPP(). *J Neurochem*.

BRACCINI, L., CIRAOLO, E., CAMPA, C. C., PERINO, A., LONGO, D. L., TIBOLLA, G., PREGNOLATO, M., CAO, Y., TASSONE, B., DAMILANO, F., LAFFARGUE, M., CALAUTTI, E., FALASCA, M., NORATA, G. D., BACKER, J. M. & HIRSCH, E. 2015. PI3K-C2gamma is a Rab5 effector selectively controlling endosomal Akt2 activation downstream of insulin signalling. *Nat Commun,* 6**,** 7400.

CALLEJA, V., ALCOR, D., LAGUERRE, M., PARK, J., VOJNOVIC, B., HEMMINGS, B. A., DOWNWARD, J., PARKER, P. J. & LARIJANI, B. 2007. Intramolecular and intermolecular interactions of protein kinase B define its activation in vivo. *PLoS Biol,* 5**,** e95.

CAO, M., WU, Y., ASHRAFI, G., MCCARTNEY, A. J., WHEELER, H., BUSHONG, E. A., BOASSA, D., ELLISMAN, M. H., RYAN, T. A. & DE CAMILLI, P. 2017. Parkinson Sac Domain Mutation in Synaptojanin 1 Impairs Clathrin Uncoating at Synapses and Triggers Dystrophic Changes in Dopaminergic Axons. *Neuron,* 93**,** 882-896.e5.

CASAMAYOR, A., MORRICE, N. A. & ALESSI, D. R. 1999. Phosphorylation of Ser-241 is essential for the activity of 3-phosphoinositide-dependent protein kinase-1: identification of five sites of phosphorylation in vivo. *Biochem J,* 342 ( Pt 2)**,** 287-92.

CASTEL, P., ELLIS, H., BAGO, R., TOSKA, E., RAZAVI, P., CARMONA, F. J., KANNAN, S., VERMA, C. S., DICKLER, M., CHANDARLAPATY, S., BROGI, E., ALESSI, D. R., BASELGA, J. & SCALTRITI, M. 2016. PDK1-SGK1 Signaling Sustains AKT-Independent mTORC1 Activation and Confers Resistance to PI3Kalpha Inhibition. *Cancer Cell,* 30**,** 229-242.

CHAGPAR, R. B., LINKS, P. H., PASTOR, M. C., FURBER, L. A., HAWRYSH, A. D., CHAMBERLAIN, M. D. & ANDERSON, D. H. 2010. Direct positive regulation of PTEN by the p85 subunit of phosphatidylinositol 3-kinase. *Proc Natl Acad Sci U S A,* 107**,** 5471-6.

CHEUNG, L. W., WALKIEWICZ, K. W., BESONG, T. M., GUO, H., HAWKE, D. H., AROLD, S. T. & MILLS, G. B. 2015. Regulation of the PI3K pathway through a p85alpha monomer-homodimer equilibrium. *Elife,* 4**,** e06866.

CHIU, R., NOVIKOV, L., MUKHERJEE, S. & SHIELDS, D. 2002. A caspase cleavage fragment of p115 induces fragmentation of the Golgi apparatus and apoptosis. *J Cell Biol,* 159**,** 637-48.
CHU, N., SALGUERO, A. L., LIU, A. Z., CHEN, Z., DEMPSEY, D. R., FICARRO, S. B., ALEXANDER, W. M., MARTO, J. A., LI, Y., AMZEL, L. M., GABELLI, S. B. & COLE, P. A. 2018. Akt Kinase Activation Mechanisms Revealed Using Protein Semisynthesis. *Cell,* 174**,** 897-907.e14.
CHUANG, C. L., LU, Y. N., WANG, H. C. & CHANG, H. Y. 2014. Genetic dissection reveals that Akt is the critical kinase downstream of LRRK2 to phosphorylate and inhibit FOXO1, and promotes neuron survival. *Hum Mol Genet,* 23**,** 5649-58.
CLARK, J., ANDERSON, K. E., JUVIN, V., SMITH, T. S., KARPE, F., WAKELAM, M. J., STEPHENS, L. R. & HAWKINS, P. T. 2011. Quantification of PtdInsP3 molecular species in cells and tissues by mass spectrometry. *Nat Methods,* 8**,** 267-72.
CONTRERAS-ZARATE, M. J., NINO, A., ROJAS, L., ARBOLEDA, H. & ARBOLEDA, G. 2015. Silencing of PINK1 inhibits insulin-like growth factor-1-mediated receptor activation and neuronal survival. *J Mol Neurosci,* 56**,** 188-97.
DAGDA, R. K., CHERRA, S. J., 3RD, KULICH, S. M., TANDON, A., PARK, D. & CHU, C. T. 2009. Loss of PINK1 function promotes mitophagy through effects on oxidative stress and mitochondrial fission. *J Biol Chem,* 284**,** 13843-55.
DAGDA, R. K., PIEN, I., WANG, R., ZHU, J., WANG, K. Z., CALLIO, J., BANERJEE, T. D., DAGDA, R. Y. & CHU, C. T. 2014. Beyond the mitochondrion: cytosolic PINK1 remodels dendrites through protein kinase A. *J Neurochem,* 128**,** 864-77.
DEAS, E., WOOD, N. W. & PLUN-FAVREAU, H. 2011. Mitophagy and Parkinson's disease: the PINK1-parkin link. *Biochim Biophys Acta,* 1813**,** 623-33.
DICKEY, A. S. & STRACK, S. 2011. PKA/AKAP1 and PP2A/Bbeta2 regulate neuronal morphogenesis via Drp1 phosphorylation and mitochondrial bioenergetics. *J Neurosci,* 31**,** 15716-26.
EBNER, M., LUCIC, I., LEONARD, T. A. & YUDUSHKIN, I. 2017. PI(3,4,5)P3 Engagement Restricts Akt Activity to Cellular Membranes. *Mol Cell,* 65**,** 416-431.e6.
ELLIS, G. I., ZHI, L., AKUNDI, R., BUELER, H. & MARTI, F. 2013. Mitochondrial and cytosolic roles of PINK1 shape induced regulatory T-cell development and function. *Eur J Immunol,* 43**,** 3355-60.
FALLON, L., BELANGER, C. M., CORERA, A. T., KONTOGIANNEA, M., REGAN-KLAPISZ, E., MOREAU, F., VOORTMAN, J., HABER, M., ROULEAU, G., THORARINSDOTTIR, T., BRICE, A., VAN BERGEN EN HENEGOUWEN, P. M. & FON, E. A. 2006. A regulated interaction with the UIM protein Eps15 implicates parkin in EGF receptor trafficking and PI(3)K-Akt signalling. *Nat Cell Biol,* 8**,** 834-42.
FAN, J., HU, Z., ZENG, L., LU, W., TANG, X., ZHANG, J. & LI, T. 2008. Golgi apparatus and neurodegenerative diseases. *Int J Dev Neurosci,* 26**,** 523-34.
FEDOROWICZ, M. A., DE VRIES-SCHNEIDER, R. L., RUB, C., BECKER, D., HUANG, Y., ZHOU, C., ALESSI WOLKEN, D. M., VOOS, W., LIU, Y. & PRZEDBORSKI, S. 2014. Cytosolic cleaved PINK1 represses Parkin translocation to mitochondria and mitophagy. *EMBO Rep,* 15**,** 86-93.
FUJITA, Y., OHAMA, E., TAKATAMA, M., AL-SARRAJ, S. & OKAMOTO, K. 2006. Fragmentation of Golgi apparatus of nigral neurons with alpha-synuclein-positive inclusions in patients with Parkinson's disease. *Acta Neuropathol,* 112**,** 261-5.
GLASL, L., KLOOS, K., GIESERT, F., ROETHIG, A., DI BENEDETTO, B., KUHN, R., ZHANG, J., HAFEN, U., ZERLE, J., HOFMANN, A., DE ANGELIS, M. H., WINKLHOFER, K. F., HOLTER, S. M., VOGT WEISENHORN, D. M. & WURST, W. 2012. Pink1-deficiency in mice impairs gait, olfaction and serotonergic innervation of the olfactory bulb. *Exp Neurol,* 235**,** 214-27.
GOSAVI, N., LEE, H. J., LEE, J. S., PATEL, S. & LEE, S. J. 2002. Golgi fragmentation occurs in the cells with prefibrillar alpha-synuclein aggregates and precedes the formation of fibrillar inclusion. *J Biol Chem,* 277**,** 48984-92.
GRIFFIN, R. J., MOLONEY, A., KELLIHER, M., JOHNSTON, J. A., RAVID, R., DOCKERY, P., O'CONNOR, R. & O'NEILL, C. 2005. Activation of Akt/PKB, increased phosphorylation of Akt substrates and

loss and altered distribution of Akt and PTEN are features of Alzheimer's disease pathology. *J Neurochem,* 93**,** 105-17.

GUPTA, A., ANJOMANI-VIRMOUNI, S., KOUNDOUROS, N., DIMITRIADI, M., CHOO-WING, R., VALLE, A., ZHENG, Y., CHIU, Y. H., AGNIHOTRI, S., ZADEH, G., ASARA, J. M., ANASTASIOU, D., ARENDS, M. J., CANTLEY, L. C. & POULOGIANNIS, G. 2017. PARK2 Depletion Connects Energy and Oxidative Stress to PI3K/Akt Activation via PTEN S-Nitrosylation. *Mol Cell,* 65**,** 999-1013.e7.

HALL, B. A., KIM, T. Y., SKOR, M. N. & CONZEN, S. D. 2012. Serum and glucocorticoid-regulated kinase 1 (SGK1) activation in breast cancer: requirement for mTORC1 activity associates with ER-alpha expression. *Breast Cancer Res Treat,* 135**,** 469-79.

HAQUE, M. E., THOMAS, K. J., D'SOUZA, C., CALLAGHAN, S., KITADA, T., SLACK, R. S., FRASER, P., COOKSON, M. R., TANDON, A. & PARK, D. S. 2008. Cytoplasmic Pink1 activity protects neurons from dopaminergic neurotoxin MPTP. *Proc Natl Acad Sci U S A,* 105**,** 1716-21.

HARPER, J. W., ORDUREAU, A. & HEO, J. M. 2018. Building and decoding ubiquitin chains for mitophagy. *Nat Rev Mol Cell Biol,* 19**,** 93-108.

HAUSER, D. N., MAMAIS, A., CONTI, M. M., PRIMIANI, C. T., KUMARAN, R., DILLMAN, A. A., LANGSTON, R. G., BEILINA, A., GARCIA, J. H., DIAZ-RUIZ, A., BERNIER, M., FIESEL, F. C., HOU, X., SPRINGER, W., LI, Y., DE CABO, R. & COOKSON, M. R. 2017. Hexokinases link DJ-1 to the PINK1/parkin pathway. *Mol Neurodegener,* 12**,** 70.

HERS, I., VINCENT, E. E. & TAVARE, J. M. 2011. Akt signalling in health and disease. *Cell Signal,* 23**,** 1515-27.

IBRAHIM, W. W., ABDELKADER, N. F., ISMAIL, H. M. & KHATTAB, M. M. 2019. Escitalopram Ameliorates Cognitive Impairment in D-Galactose-Injected Ovariectomized Rats: Modulation of JNK, GSK-3beta, and ERK Signalling Pathways. *Sci Rep,* 9**,** 10056.

JARAMILLO-GOMEZ, J., NINO, A., ARBOLEDA, H. & ARBOLEDA, G. 2015. Overexpression of DJ-1 protects against C2-ceramide-induced neuronal death through activation of the PI3K/AKT pathway and inhibition of autophagy. *Neurosci Lett,* 603**,** 71-6.

JETHWA, N., CHUNG, G. H., LETE, M. G., ALONSO, A., BYRNE, R. D., CALLEJA, V. & LARIJANI, B. 2015. Endomembrane PtdIns(3,4,5)P3 activates the PI3K-Akt pathway. *J Cell Sci,* 128**,** 3456-65.

KANE, L. A., LAZAROU, M., FOGEL, A. I., LI, Y., YAMANO, K., SARRAF, S. A., BANERJEE, S. & YOULE, R. J. 2014. PINK1 phosphorylates ubiquitin to activate Parkin E3 ubiquitin ligase activity. *J Cell Biol,* 205**,** 143-53.

KAWAJIRI, S., SAIKI, S., SATO, S., SATO, F., HATANO, T., EGUCHI, H. & HATTORI, N. 2010. PINK1 is recruited to mitochondria with parkin and associates with LC3 in mitophagy. *FEBS Lett,* 584**,** 1073-9.

KAZLAUSKAITE, A., KONDAPALLI, C., GOURLAY, R., CAMPBELL, D. G., RITORTO, M. S., HOFMANN, K., ALESSI, D. R., KNEBEL, A., TROST, M. & MUQIT, M. M. 2014. Parkin is activated by PINK1-dependent phosphorylation of ubiquitin at Ser65. *Biochem J,* 460**,** 127-39.

KIELKOWSKA, A., NIEWCZAS, I., ANDERSON, K. E., DURRANT, T. N., CLARK, J., STEPHENS, L. R. & HAWKINS, P. T. 2014. A new approach to measuring phosphoinositides in cells by mass spectrometry. *Adv Biol Regul,* 54**,** 131-41.

KIM, R. H., PETERS, M., JANG, Y., SHI, W., PINTILIE, M., FLETCHER, G. C., DELUCA, C., LIEPA, J., ZHOU, L., SNOW, B., BINARI, R. C., MANOUKIAN, A. S., BRAY, M. R., LIU, F. F., TSAO, M. S. & MAK, T. W. 2005. DJ-1, a novel regulator of the tumor suppressor PTEN. *Cancer Cell,* 7**,** 263-73.

KIM, S. R., CHEN, X., OO, T. F., KAREVA, T., YARYGINA, O., WANG, C., DURING, M., KHOLODILOV, N. & BURKE, R. E. 2011. Dopaminergic pathway reconstruction by Akt/Rheb-induced axon regeneration. *Ann Neurol,* 70**,** 110-20.

KOMANDER, D., KULAR, G., DEAK, M., ALESSI, D. R. & VAN AALTEN, D. M. 2005. Role of T-loop phosphorylation in PDK1 activation, stability, and substrate binding. *J Biol Chem,* 280**,** 18797-802.

KONDAPALLI, C., KAZLAUSKAITE, A., ZHANG, N., WOODROOF, H. I., CAMPBELL, D. G., GOURLAY, R., BURCHELL, L., WALDEN, H., MACARTNEY, T. J., DEAK, M., KNEBEL, A., ALESSI, D. R. & MUQIT, M. M. 2012. PINK1 is activated by mitochondrial membrane potential depolarization and stimulates Parkin E3 ligase activity by phosphorylating Serine 65. *Open Biol,* 2**,** 120080.

KOYANO, F., OKATSU, K., KOSAKO, H., TAMURA, Y., GO, E., KIMURA, M., KIMURA, Y., TSUCHIYA, H., YOSHIHARA, H., HIROKAWA, T., ENDO, T., FON, E. A., TREMPE, J. F., SAEKI, Y., TANAKA, K. & MATSUDA, N. 2014. Ubiquitin is phosphorylated by PINK1 to activate parkin. *Nature,* 510**,** 162-6.

KREBS, C. E., KARKHEIRAN, S., POWELL, J. C., CAO, M., MAKAROV, V., DARVISH, H., DI PAOLO, G., WALKER, R. H., SHAHIDI, G. A., BUXBAUM, J. D., DE CAMILLI, P., YUE, Z. & PAISAN-RUIZ, C. 2013. The Sac1 domain of SYNJ1 identified mutated in a family with early-onset progressive Parkinsonism with generalized seizures. *Hum Mutat,* 34**,** 1200-7.

KUTATELADZE, T. G. 2010. Translation of the phosphoinositide code by PI effectors. *Nat Chem Biol,* 6**,** 507-13.

LANE, J. D., LUCOCQ, J., PRYDE, J., BARR, F. A., WOODMAN, P. G., ALLAN, V. J. & LOWE, M. 2002. Caspase-mediated cleavage of the stacking protein GRASP65 is required for Golgi fragmentation during apoptosis. *J Cell Biol,* 156**,** 495-509.

LEE, H. J. & CHUNG, K. C. 2012. PINK1 positively regulates IL-1beta-mediated signaling through Tollip and IRAK1 modulation. *J Neuroinflammation,* 9**,** 271.

LEE, H. J., JANG, S. H., KIM, H., YOON, J. H. & CHUNG, K. C. 2012. PINK1 stimulates interleukin-1beta-mediated inflammatory signaling via the positive regulation of TRAF6 and TAK1. *Cell Mol Life Sci,* 69**,** 3301-15.

LI, Y., QIU, L., LIU, X., HOU, Z. & YU, B. 2017. PINK1 alleviates myocardial hypoxia-reoxygenation injury by ameliorating mitochondrial dysfunction. *Biochem Biophys Res Commun,* 484**,** 118-124.

LINDSAY, A. J., JOLLIVET, F., HORGAN, C. P., KHAN, A. R., RAPOSO, G., MCCAFFREY, M. W. & GOUD, B. 2013. Identification and characterization of multiple novel Rab-myosin Va interactions. *Mol Biol Cell,* 24**,** 3420-34.

LINDSAY, A. J. & MCCAFFREY, M. W. 2009. Myosin Vb localises to nucleoli and associates with the RNA polymerase I transcription complex. *Cell Motil Cytoskeleton,* 66**,** 1057-72.

LUCIC, I., RATHINASWAMY, M. K., TRUEBESTEIN, L., HAMELIN, D. J., BURKE, J. E. & LEONARD, T. A. 2018. Conformational sampling of membranes by Akt controls its activation and inactivation. *Proc Natl Acad Sci U S A,* 115**,** E3940-e3949.

MACHAMER, C. E. 2003. Golgi disassembly in apoptosis: cause or effect? *Trends Cell Biol,* 13**,** 279-81.

MACKEIGAN, J. P., MURPHY, L. O. & BLENIS, J. 2005. Sensitized RNAi screen of human kinases and phosphatases identifies new regulators of apoptosis and chemoresistance. *Nat Cell Biol,* 7**,** 591-600.

MAEHAMA, T. & DIXON, J. E. 1998. The tumor suppressor, PTEN/MMAC1, dephosphorylates the lipid second messenger, phosphatidylinositol 3,4,5-trisphosphate. *J Biol Chem,* 273**,** 13375-8.

MAJ, M. C., TKACHYOVA, I., PATEL, P., ADDIS, J. B., MACKAY, N., LEVANDOVSKIY, V., LEE, J., LANG, A. E., CAMERON, J. M. & ROBINSON, B. H. 2010. Oxidative stress alters the regulatory control of p66Shc and Akt in PINK1 deficient cells. *Biochem Biophys Res Commun,* 399**,** 331-5.

MALAGELADA, C., JIN, Z. H. & GREENE, L. A. 2008. RTP801 is induced in Parkinson's disease and mediates neuron death by inhibiting Akt phosphorylation/activation. *J Neurosci,* 28**,** 14363-71.

MANNING, B. D. & TOKER, A. 2017. AKT/PKB Signaling: Navigating the Network. *Cell,* 169**,** 381-405.

MATHEOUD, D., SUGIURA, A., BELLEMARE-PELLETIER, A., LAPLANTE, A., RONDEAU, C., CHEMALI, M., FAZEL, A., BERGERON, J. J., TRUDEAU, L. E., BURELLE, Y., GAGNON, E., MCBRIDE, H. M. & DESJARDINS, M. 2016. Parkinson's Disease-Related Proteins PINK1 and Parkin Repress Mitochondrial Antigen Presentation. *Cell,* 166**,** 314-327.

MATSUDA, N., SATO, S., SHIBA, K., OKATSU, K., SAISHO, K., GAUTIER, C. A., SOU, Y. S., SAIKI, S., KAWAJIRI, S., SATO, F., KIMURA, M., KOMATSU, M., HATTORI, N. & TANAKA, K. 2010. PINK1 stabilized by mitochondrial depolarization recruits Parkin to damaged mitochondria and activates latent Parkin for mitophagy. *J Cell Biol,* 189**,** 211-21.

MCCOY, M. K., KAGANOVICH, A., RUDENKO, I. N., DING, J. & COOKSON, M. R. 2014. Hexokinase activity is required for recruitment of parkin to depolarized mitochondria. *Hum Mol Genet,* 23**,** 145-56.

MEI, Y., ZHANG, Y., YAMAMOTO, K., XIE, W., MAK, T. W. & YOU, H. 2009. FOXO3a-dependent regulation of Pink1 (Park6) mediates survival signaling in response to cytokine deprivation. *Proc Natl Acad Sci U S A,* 106**,** 5153-8.

MEYER, R., D'ALESSANDRO, L. A., KAR, S., KRAMER, B., SHE, B., KASCHEK, D., HAHN, B., WRANGBORG, D., KARLSSON, J., KVARNSTROM, M., JIRSTRAND, M., LEHMANN, W. D., TIMMER, J., HOFER, T. & KLINGMULLER, U. 2012. Heterogeneous kinetics of AKT signaling in individual cells are accounted for by variable protein concentration. *Front Physiol,* 3**,** 451.

MOLONEY, A. M., GRIFFIN, R. J., TIMMONS, S., O'CONNOR, R., RAVID, R. & O'NEILL, C. 2010. Defects in IGF-1 receptor, insulin receptor and IRS-1/2 in Alzheimer's disease indicate possible resistance to IGF-1 and insulin signalling. *Neurobiol Aging,* 31**,** 224-43.

MORAIS, V. A., VERSTREKEN, P., ROETHIG, A., SMET, J., SNELLINX, A., VANBRABANT, M., HADDAD, D., FREZZA, C., MANDEMAKERS, W., VOGT-WEISENHORN, D., VAN COSTER, R., WURST, W., SCORRANO, L. & DE STROOPER, B. 2009. Parkinson's disease mutations in PINK1 result in decreased Complex I activity and deficient synaptic function. *EMBO Mol Med,* 1**,** 99-111.

MOULT, P. R., CROSS, A., SANTOS, S. D., CARVALHO, A. L., LINDSAY, Y., CONNOLLY, C. N., IRVING, A. J., LESLIE, N. R. & HARVEY, J. 2010. Leptin regulates AMPA receptor trafficking via PTEN inhibition. *J Neurosci,* 30**,** 4088-101.

MURATA, H., SAKAGUCHI, M., JIN, Y., SAKAGUCHI, Y., FUTAMI, J., YAMADA, H., KATAOKA, K. & HUH, N. H. 2011. A new cytosolic pathway from a Parkinson disease-associated kinase, BRPK/PINK1: activation of AKT via mTORC2. *J Biol Chem,* 286**,** 7182-9.

NAKAGOMI, S., BARSOUM, M. J., BOSSY-WETZEL, E., SUTTERLIN, C., MALHOTRA, V. & LIPTON, S. A. 2008. A Golgi fragmentation pathway in neurodegeneration. *Neurobiol Dis,* 29**,** 221-31.

O'FLANAGAN, C. H., MORAIS, V. A., WURST, W., DE STROOPER, B. & O'NEILL, C. 2015. The Parkinson's gene PINK1 regulates cell cycle progression and promotes cancer-associated phenotypes. *Oncogene,* 34**,** 1363-74.

O'FLANAGAN, C. H. & O'NEILL, C. 2014. PINK1 signalling in cancer biology. *Biochim Biophys Acta,* 1846**,** 590-8.

OHTA, E., KAWAKAMI, F., KUBO, M. & OBATA, F. 2011. LRRK2 directly phosphorylates Akt1 as a possible physiological substrate: impairment of the kinase activity by Parkinson's disease-associated mutations. *FEBS Lett,* 585**,** 2165-70.

PAPAKONSTANTI, E. A., RIDLEY, A. J. & VANHAESEBROECK, B. 2007. The p110delta isoform of PI 3-kinase negatively controls RhoA and PTEN. *Embo j,* 26**,** 3050-61.

PEDROSA, A. R., BODRUG, N., GOMEZ-ESCUDERO, J., CARTER, E. P., REYNOLDS, L. E., GEORGIOU, P. N., FERNANDEZ, I., LEES, D. M., KOSTOUROU, V., ALEXOPOULOU, A. N., BATISTA, S., TAVORA, B., SERRELS, B., PARSONS, M., ISKRATSCH, T. & HODIVALA-DILKE, K. M. 2019. Tumor angiogenesis is differentially regulated by phosphorylation of endothelial cell focal adhesion kinase tyrosines-397 and -861. *Cancer Res*.

PENG, W., LEI, Q., JIANG, Z. & HU, Z. 2014. Characterization of Golgi scaffold proteins and their roles in compartmentalizing cell signaling. *J Mol Histol,* 45**,** 435-45.

PILSL, A. & WINKLHOFER, K. F. 2012. Parkin, PINK1 and mitochondrial integrity: emerging concepts of mitochondrial dysfunction in Parkinson's disease. *Acta Neuropathol,* 123**,** 173-88.

PRIDGEON, J. W., OLZMANN, J. A., CHIN, L. S. & LI, L. 2007. PINK1 protects against oxidative stress by phosphorylating mitochondrial chaperone TRAP1. *PLoS Biol,* 5**,** e172.

RABINOVSKY, R., POCHANARD, P., MCNEAR, C., BRACHMANN, S. M., DUKE-COHAN, J. S., GARRAWAY, L. A. & SELLERS, W. R. 2009. p85 Associates with unphosphorylated PTEN and the PTEN-associated complex. *Mol Cell Biol,* 29**,** 5377-88.

RENDON, W. O., MARTINEZ-ALONSO, E., TOMAS, M., MARTINEZ-MARTINEZ, N. & MARTINEZ-MENARGUEZ, J. A. 2013. Golgi fragmentation is Rab and SNARE dependent in cellular models of Parkinson's disease. *Histochem Cell Biol,* 139**,** 671-84.

RIES, V., HENCHCLIFFE, C., KAREVA, T., RZHETSKAYA, M., BLAND, R., DURING, M. J., KHOLODILOV, N. & BURKE, R. E. 2006. Oncoprotein Akt/PKB induces trophic effects in murine models of Parkinson's disease. *Proc Natl Acad Sci U S A,* 103**,** 18757-62.

SALAMON, R. S. & BACKER, J. M. 2013. Phosphatidylinositol-3,4,5-trisphosphate: tool of choice for class I PI 3-kinases. *Bioessays,* 35**,** 602-11.

SANCHEZ-MORA, R. M., ARBOLEDA, H. & ARBOLEDA, G. 2012. PINK1 overexpression protects against C2-ceramide-induced CAD cell death through the PI3K/AKT pathway. *J Mol Neurosci,* 47**,** 582-94.

SANDEBRING, A., THOMAS, K. J., BEILINA, A., VAN DER BRUG, M., CLELAND, M. M., AHMAD, R., MILLER, D. W., ZAMBRANO, I., COWBURN, R. F., BEHBAHANI, H., CEDAZO-MINGUEZ, A. & COOKSON, M. R. 2009. Mitochondrial alterations in PINK1 deficient cells are influenced by calcineurin-dependent dephosphorylation of dynamin-related protein 1. *PLoS One,* 4**,** e5701.

SARBASSOV, D. D., ALI, S. M., KIM, D. H., GUERTIN, D. A., LATEK, R. R., ERDJUMENT-BROMAGE, H., TEMPST, P. & SABATINI, D. M. 2004. Rictor, a novel binding partner of mTOR, defines a rapamycin-insensitive and raptor-independent pathway that regulates the cytoskeleton. *Curr Biol,* 14**,** 1296-302.

SARBASSOV, D. D., GUERTIN, D. A., ALI, S. M. & SABATINI, D. M. 2005. Phosphorylation and regulation of Akt/PKB by the rictor-mTOR complex. *Science,* 307**,** 1098-101.

SATO, M., UEDA, Y., TAKAGI, T. & UMEZAWA, Y. 2003. Production of PtdInsP3 at endomembranes is triggered by receptor endocytosis. *Nat Cell Biol,* 5**,** 1016-22.

SEO, J. H., RAH, J. C., CHOI, S. H., SHIN, J. K., MIN, K., KIM, H. S., PARK, C. H., KIM, S., KIM, E. M., LEE, S. H., LEE, S., SUH, S. W. & SUH, Y. H. 2002. Alpha-synuclein regulates neuronal survival via Bcl-2 family expression and PI3/Akt kinase pathway. *Faseb j,* 16**,** 1826-8.

SHA, D., CHIN, L. S. & LI, L. 2010. Phosphorylation of parkin by Parkinson disease-linked kinase PINK1 activates parkin E3 ligase function and NF-kappaB signaling. *Hum Mol Genet,* 19**,** 352-63.

SHIBA-FUKUSHIMA, K., IMAI, Y., YOSHIDA, S., ISHIHAMA, Y., KANAO, T., SATO, S. & HATTORI, N. 2012. PINK1-mediated phosphorylation of the Parkin ubiquitin-like domain primes mitochondrial translocation of Parkin and regulates mitophagy. *Sci Rep,* 2**,** 1002.

SIDDHANTA, A., RADULESCU, A., STANKEWICH, M. C., MORROW, J. S. & SHIELDS, D. 2003. Fragmentation of the Golgi apparatus. A role for beta III spectrin and synthesis of phosphatidylinositol 4,5-bisphosphate. *J Biol Chem,* 278**,** 1957-65.

SOUTAR, M. P. M., KEMPTHORNE, L., MIYAKAWA, S., ANNUARIO, E., MELANDRI, D., HARLEY, J., O'SULLIVAN, G. A., WRAY, S., HANCOCK, D. C., COOKSON, M. R., DOWNWARD, J., CARLTON, M. & PLUN-FAVREAU, H. 2018. AKT signalling selectively regulates PINK1 mitophagy in SHSY5Y cells and human iPSC-derived neurons. *Sci Rep,* 8**,** 8855.

STEER, E. K., DAIL, M. K. & CHU, C. T. 2015. Beyond mitophagy: cytosolic PINK1 as a messenger of mitochondrial health. *Antioxid Redox Signal,* 22**,** 1047-59.

STOKOE, D., STEPHENS, L. R., COPELAND, T., GAFFNEY, P. R., REESE, C. B., PAINTER, G. F., HOLMES, A. B., MCCORMICK, F. & HAWKINS, P. T. 1997. Dual role of phosphatidylinositol-3,4,5-trisphosphate in the activation of protein kinase B. *Science,* 277**,** 567-70.

THORPE, L. M., SPANGLE, J. M., OHLSON, C. E., CHENG, H., ROBERTS, T. M., CANTLEY, L. C. & ZHAO, J. J. 2017. PI3K-p110alpha mediates the oncogenic activity induced by loss of the novel tumor suppressor PI3K-p85alpha. *Proc Natl Acad Sci U S A,* 114**,** 7095-7100.

TIMMONS, S., COAKLEY, M. F., MOLONEY, A. M. & C, O. N. 2009. Akt signal transduction dysfunction in Parkinson's disease. *Neurosci Lett,* 467**,** 30-5.

TSOLAKOS, N., DURRANT, T. N., CHESSA, T., SUIRE, S. M., OXLEY, D., KULKARNI, S., DOWNWARD, J., PERISIC, O., WILLIAMS, R. L., STEPHENS, L. & HAWKINS, P. T. 2018. Quantitation of class IA PI3Ks in mice reveals p110-free-p85s and isoform-selective subunit associations and recruitment to receptors. *Proc Natl Acad Sci U S A,* 115**,** 12176-12181.

UNOKI, M. & NAKAMURA, Y. 2001. Growth-suppressive effects of BPOZ and EGR2, two genes involved in the PTEN signaling pathway. *Oncogene,* 20**,** 4457-65.

VALENTE, E. M., ABOU-SLEIMAN, P. M., CAPUTO, V., MUQIT, M. M., HARVEY, K., GISPERT, S., ALI, Z., DEL TURCO, D., BENTIVOGLIO, A. R., HEALY, D. G., ALBANESE, A., NUSSBAUM, R., GONZALEZ-MALDONADO, R., DELLER, T., SALVI, S., CORTELLI, P., GILKS, W. P., LATCHMAN, D. S., HARVEY, R. J., DALLAPICCOLA, B., AUBURGER, G. & WOOD, N. W. 2004. Hereditary early-onset Parkinson's disease caused by mutations in PINK1. *Science,* 304**,** 1158-60.

VANHAUWAERT, R., KUENEN, S., MASIUS, R., BADEMOSI, A., MANETSBERGER, J., SCHOOVAERTS, N., BOUNTI, L., GONTCHARENKO, S., SWERTS, J., VILAIN, S., PICILLO, M., BARONE, P., MUNSHI, S. T., DE VRIJ, F. M., KUSHNER, S. A., GOUNKO, N. V., MANDEMAKERS, W., BONIFATI, V., MEUNIER, F. A., SOUKUP, S. F. & VERSTREKEN, P. 2017. The SAC1 domain in synaptojanin is required for autophagosome maturation at presynaptic terminals. *Embo j,* 36**,** 1392-1411.

VINCOW, E. S., MERRIHEW, G., THOMAS, R. E., SHULMAN, N. J., BEYER, R. P., MACCOSS, M. J. & PALLANCK, L. J. 2013. The PINK1-Parkin pathway promotes both mitophagy and selective respiratory chain turnover in vivo. *Proc Natl Acad Sci U S A,* 110**,** 6400-5.

WANG, Y., WEISS, L. M. & ORLOFSKY, A. 2010. Coordinate control of host centrosome position, organelle distribution, and migratory response by Toxoplasma gondii via host mTORC2. *J Biol Chem,* 285**,** 15611-8.

WATTON, S. J. & DOWNWARD, J. 1999. Akt/PKB localisation and 3' phosphoinositide generation at sites of epithelial cell-matrix and cell-cell interaction. *Curr Biol,* 9**,** 433-6.

WENK, M. R. & DE CAMILLI, P. 2004. Protein-lipid interactions and phosphoinositide metabolism in membrane traffic: insights from vesicle recycling in nerve terminals. *Proc Natl Acad Sci U S A,* 101**,** 8262-9.

WICK, M. J., RAMOS, F. J., CHEN, H., QUON, M. J., DONG, L. Q. & LIU, F. 2003. Mouse 3-phosphoinositide-dependent protein kinase-1 undergoes dimerization and trans-phosphorylation in the activation loop. *J Biol Chem,* 278**,** 42913-9.

WOOD-KACZMAR, A., GANDHI, S., YAO, Z., ABRAMOV, A. Y., MILJAN, E. A., KEEN, G., STANYER, L., HARGREAVES, I., KLUPSCH, K., DEAS, E., DOWNWARD, J., MANSFIELD, L., JAT, P., TAYLOR, J., HEALES, S., DUCHEN, M. R., LATCHMAN, D., TABRIZI, S. J. & WOOD, N. W. 2008. PINK1 is necessary for long term survival and mitochondrial function in human dopaminergic neurons. *PLoS One,* 3**,** e2455.

XIONG, H., WANG, D., CHEN, L., CHOO, Y. S., MA, H., TANG, C., XIA, K., JIANG, W., RONAI, Z., ZHUANG, X. & ZHANG, Z. 2009. Parkin, PINK1, and DJ-1 form a ubiquitin E3 ligase complex promoting unfolded protein degradation. *J Clin Invest,* 119**,** 650-60.

YANG, J., CRON, P., GOOD, V. M., THOMPSON, V., HEMMINGS, B. A. & BARFORD, D. 2002. Crystal structure of an activated Akt/protein kinase B ternary complex with GSK3-peptide and AMP-PNP. *Nat Struct Biol,* 9**,** 940-4.

YANG, W., WANG, X., LIU, J., DUAN, C., GAO, G., LU, L., YU, S. & YANG, H. 2018. PINK1 suppresses alpha-synuclein-induced neuronal injury: a novel mechanism in protein phosphatase 2A activation. *Oncotarget,* 9**,** 37-53.

YAP, T. A., YAN, L., PATNAIK, A., FEAREN, I., OLMOS, D., PAPADOPOULOS, K., BAIRD, R. D., DELGADO, L., TAYLOR, A., LUPINACCI, L., RIISNAES, R., POPE, L. L., HEATON, S. P., THOMAS, G., GARRETT, M. D., SULLIVAN, D. M., DE BONO, J. S. & TOLCHER, A. W. 2011. First-in-man clinical trial of the oral pan-AKT inhibitor MK-2206 in patients with advanced solid tumors. *J Clin Oncol,* 29**,** 4688-95.

YOULE, R. J. & NARENDRA, D. P. 2011. Mechanisms of mitophagy. *Nat Rev Mol Cell Biol,* 12**,** 9-14.

YOULE, R. J. & VAN DER BLIEK, A. M. 2012. Mitochondrial fission, fusion, and stress. *Science,* 337**,** 1062-5.

ZHANG, Y., GONG, X. G., WANG, Z. Z., SUN, H. M., GUO, Z. Y., HU, J. H., MA, L., LI, P. & CHEN, N. H. 2016. Overexpression of DJ-1/PARK7, the Parkinson's disease-related protein, improves mitochondrial function via Akt phosphorylation on threonine 308 in dopaminergic neuron-like cells. *Eur J Neurosci,* 43**,** 1379-88.

ZHENG, J., FAN, R., WU, H., YAO, H., YAN, Y., LIU, J., RAN, L., SUN, Z., YI, L., DANG, L., GAN, P., ZHENG, P., YANG, T., ZHANG, Y., TANG, T. & WANG, Y. 2019. Directed self-assembly of herbal small molecules into sustained release hydrogels for treating neural inflammation. *Nat Commun,* 10**,** 1604.

ZIVIANI, E., TAO, R. N. & WHITWORTH, A. J. 2010. Drosophila parkin requires PINK1 for mitochondrial translocation and ubiquitinates mitofusin. *Proc Natl Acad Sci U S A,* 107**,** 5018-23.

## Figures

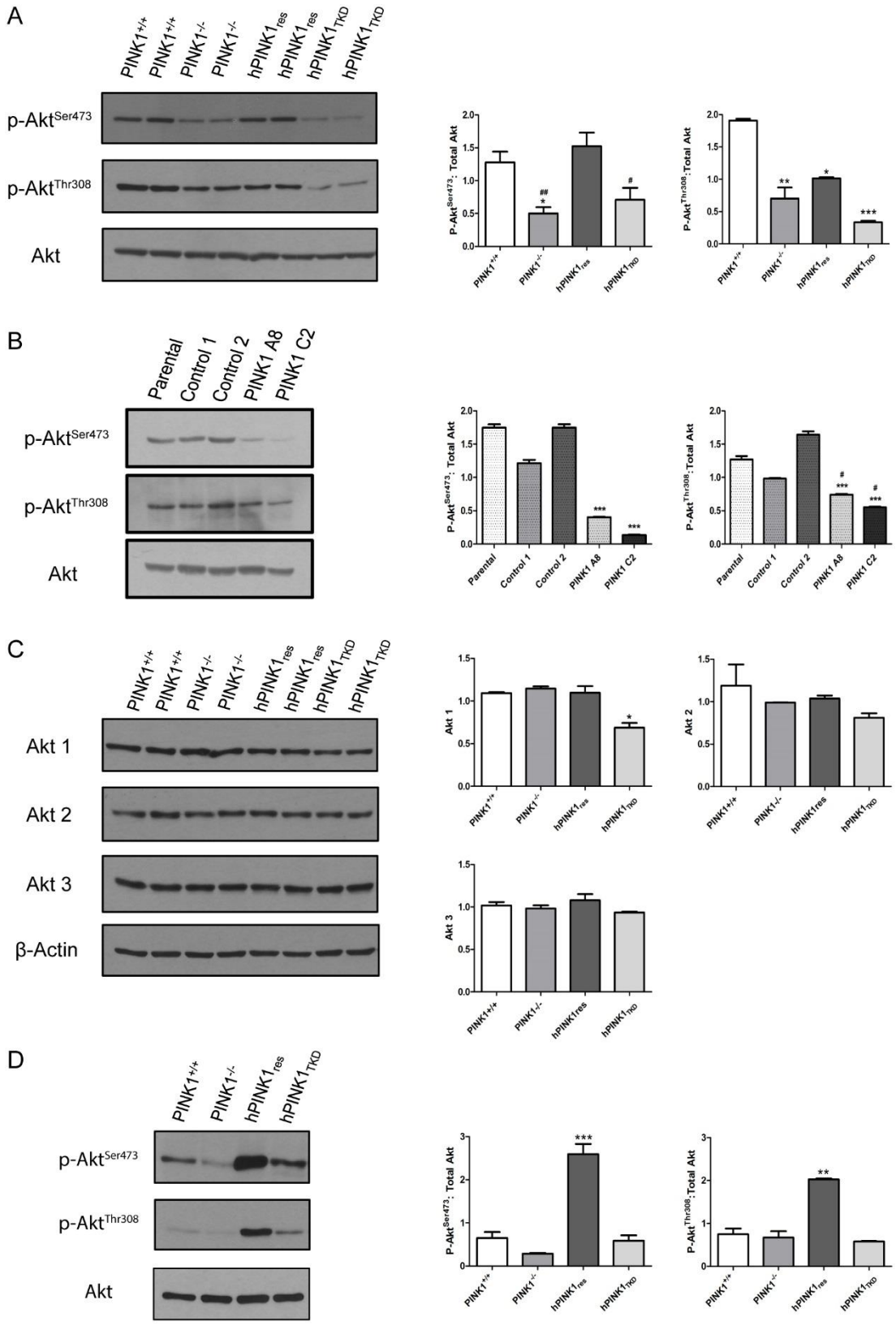

**Figure 1 PINK1 is a major regulator of Akt activation.**

A Representative immunoblot analysis showing phosphorylation of Akt at $Ser^{473}$ and $Thr^{308}$ in $PINK1^{+/+}$, $PINK1^{-/-}$, $hPINK1_{res}$ and $hPINK1_{TKD}$ MEFs, which were grown for 24h in DMEM-Hi supplemented with 10% FBS. B Representative immunoblot analysis showing phosphorylation of Akt at $Ser^{473}$ and $Thr^{308}$ in BE M17s, which were grown for 24h in DMEM-Hi supplemented with 10% FBS. C Representative immunoblot analysis showing levels of Akt 1, 2, and 3 in $PINK1^{+/+}$, $PINK1^{-/-}$, $hPINK1_{res}$ and $hPINK1_{TKD}$ MEFs, which were grown for 24h in DMEM-Hi supplemented with 10% FBS. D Representative immunoblot analysis showing phosphorylation of Akt at $Ser^{473}$ and $Thr^{308}$ in $PINK1^{+/+}$, $PINK1^{-/-}$, $hPINK1_{res}$ and $hPINK1_{TKD}$ MEFs, which were grown in the absence of serum. Data information: In A-C, data are presented in corresponding graphs as mean ± SEM (n = 3 biological replicates for each). *=p<0.05, **=p<0.01, and ***=p<0.0001 with respect to $PINK1^{+/+}$ MEFs. #=p<0.05 ##=p<0.01 with respect to $hPINK1_{res}$ MEFs (One-way ANOVA). In D, data are presented in corresponding graphs as mean ± SEM (n = 3 biological replicates). **=p<0.01, and ***=p<0.0001 with respect to $PINK1^{+/+}$, $hPINK1_{res}$ and $hPINK1_{TKD}$ MEFs.

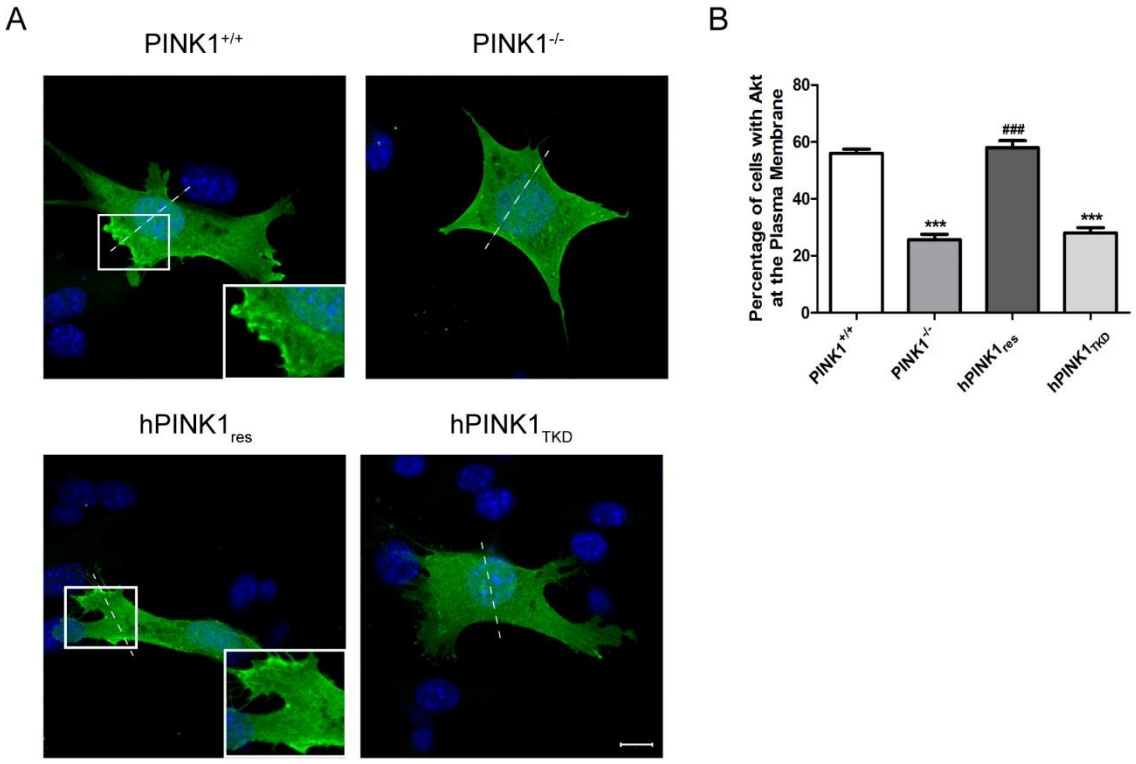


**Figure 2 PINK1 regulates the localisation of Akt to the plasma membrane.**

A Representative confocal images showing GFP-Akt-PH localisation in PINK1$^{+/+}$, PINK1$^{-/-}$, hPINK1$_{res}$ and hPINK1$_{TKD}$ MEFs, which were grown in DMEM-Hi supplemented with 10% FBS, transfected with GFP-Akt-PH for 24h and stained with DAPI (blue). Scale bars 10 μm. B Histogram depicting the percentage of transfected cells with Akt accumulations at the plasma membrane. Data information: In B data are presented as mean ± SEM (n = 3 biological replicates for each). ***=p<0.0001 with respect to PINK1$^{+/+}$ MEFs. ###=p<0.0001 with respect to PINK1$^{-/-}$ MEFs and hPINK1$_{TKD}$ MEFs (One way ANOVA).

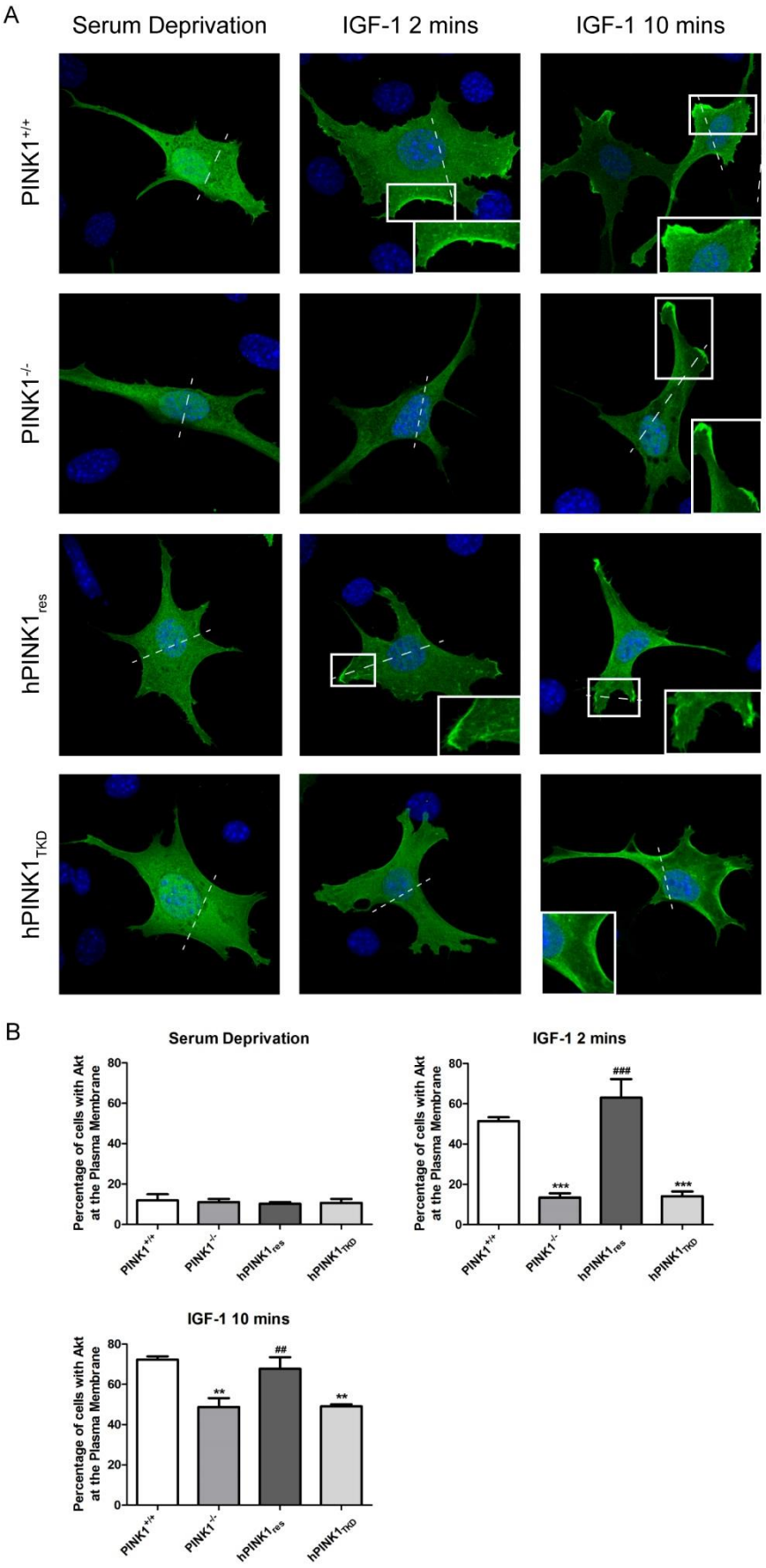

**Figure 3 PINK1 decreases the time taken for Akt to get to the plasma membrane in response to IGF-1 stimulation.**

A Representative confocal images showing GFP-Akt-PH localisation in $PINK1^{+/+}$, $PINK1^{-/-}$, $hPINK1_{res}$ and $hPINK1_{TKD}$ MEFs, following transfection with GFP-Akt-PH for 24 h and stained with DAPI (blue). Serum-starved cells were stimulated with 10 ng/ml IGF-1 for the indicated times (n = 3 biological replicates). Scale bars 10 μm. B Histograms depicting the percentage of transfected cells with Akt accumulations at the plasma membrane. Data information: In B data are presented as mean ± SEM (n = 3 biological replicates). **=p<0.01, and ***=p<0.0001 with respect to $PINK1^{+/+}$ MEFs. ##=p<0.01 and ###=p<0.0001 with respect to $PINK1^{-/-}$ and $hPINK1_{TKD}$ MEFs (One-way ANOVA).

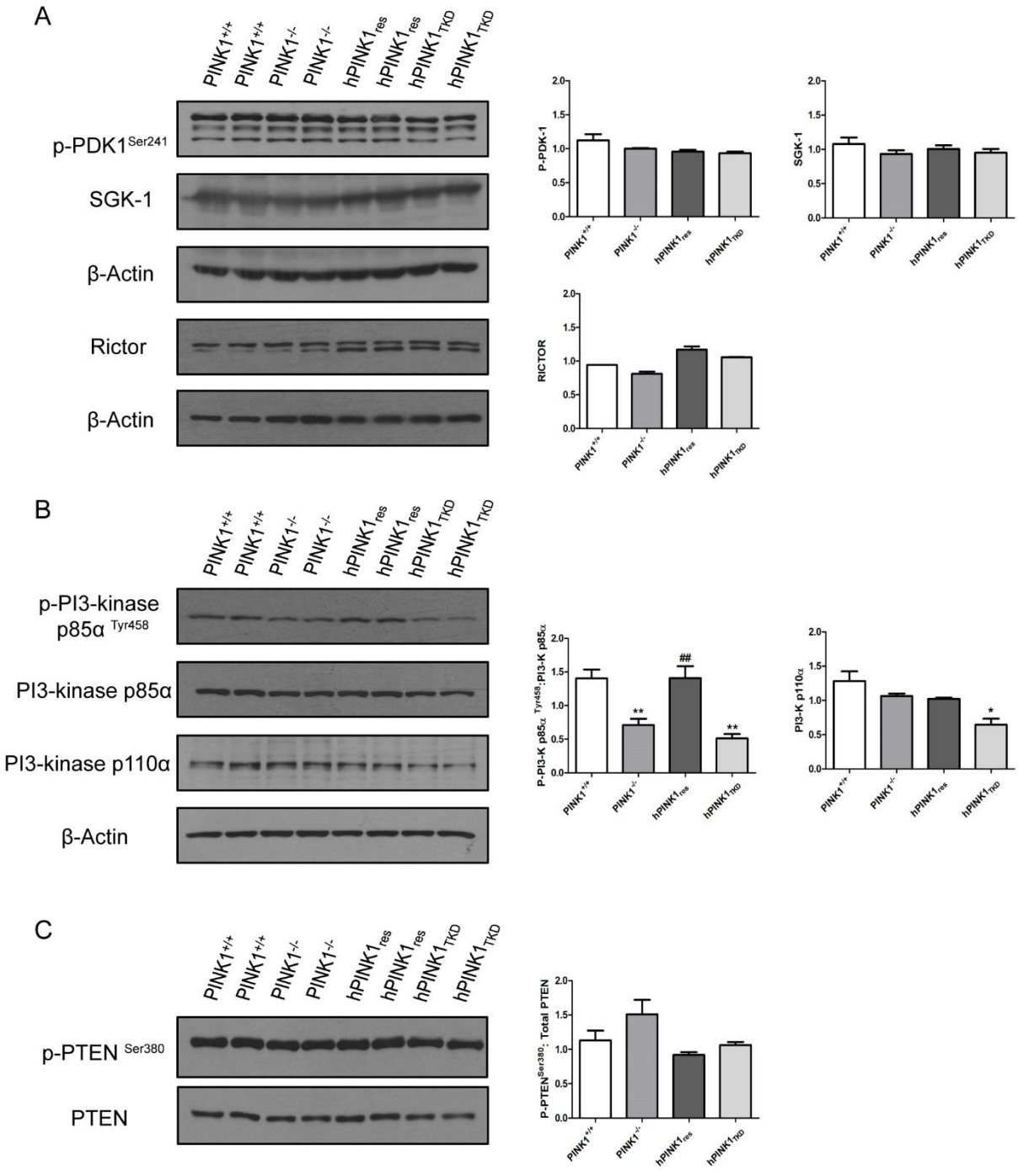


**Figure 4 Phosphorylation and activation of PI3-kinase is PINK1 kinase-dependent.**

A-C Representative immunoblot analysis showing relative expression of proteins which regulate Akt activation in PINK1$^{+/+}$, PINK1$^{-/-}$, hPINK1$_{res}$ and hPINK1$_{TKD}$ MEFs, which were grown in DMEM-Hi supplemented with 10% FBS. Data information: In A-C, data are

presented in corresponding graphs as mean ± SEM (n = 3 biological replicates for each). *=p < 0.05 and **=p < 0.01 with respect to $PINK1^{+/+}$ MEFs and ##=p < 0.01 with respect to $PINK1^{-/-}$ and $hPINK1_{TKD}$ MEFs (One-way ANOVA).

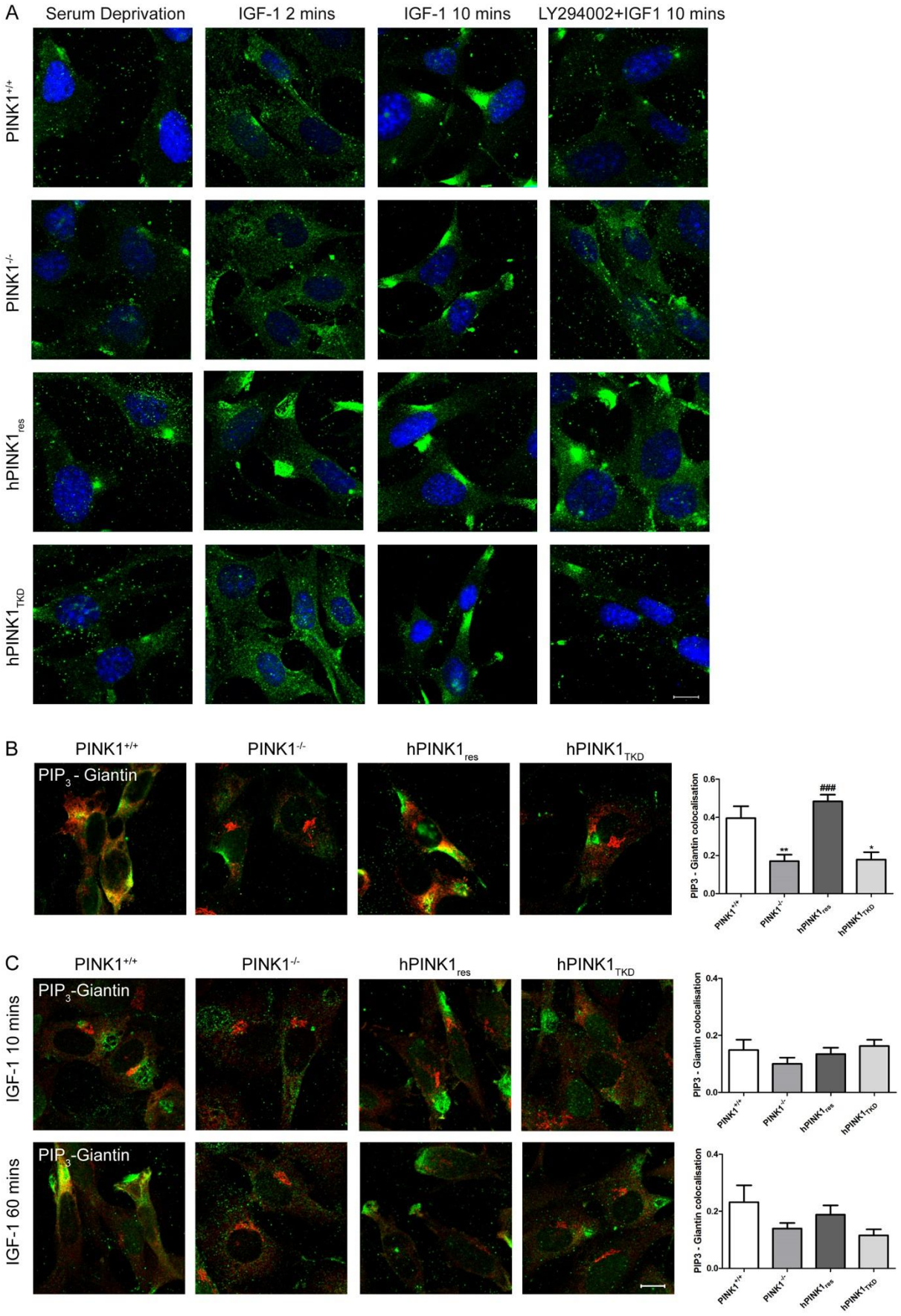

**Figure 5 $PIP_3$ localisation is PINK1 kinase-dependent.**

A Representative confocal images showing $PIP_3$ localisation in $PINK1^{+/+}$, $PINK1^{-/-}$, $hPINK1_{res}$ and $hPINK1_{TKD}$ MEFs. Serum-starved cells were stimulated with 10 ng/ml IGF-1 for the indicated times, or pre-incubated with 10 μM LY294002 and subsequently stimulated with 10 ng/ml IGF-1, and immunostained for $PIP_3$ (green) and DAPI (blue) (n = 3 biological replicates). Scale bar 10 μm. B Representative confocal images showing $PIP_3$ localisation in $PINK1^{+/+}$, $PINK1^{-/-}$, $hPINK1_{res}$ and $hPINK1_{TKD}$ MEFs, which were grown in DMEM-Hi supplemented with 10% FBS, and immunostained for $PIP_3$ (green) and Giantin (red), the accompanying histogram shows the colocalisation percentage of $PIP_3$ and Giantin in each cell type (n = 3 biological replicates). Scale bar 10 μm. C Representative confocal images showing $PIP_3$ localisation in $PINK1^{+/+}$, $PINK1^{-/-}$, $hPINK1_{res}$ and $hPINK1_{TKD}$ MEFs. Serum-starved cells were stimulated with 10 ng/ml IGF-1 for the indicated times, and immunostained for $PIP_3$ (green) and Giantin (red), the accompanying histogram shows the colocalisation percentage of $PIP_3$ and Giantin (n = 3 biological replicates). Scale bar 10 μm. Data information: In B and C, data are presented as mean ± SEM. *=$p < 0.05$, **=$p < 0.01$ with respect to $PINK1^{+/+}$ MEFs and $hPINK1_{res}$ MEFs, ###=$p < 0.0001$ with respect to $PINK1^{-/-}$ MEFs (One-way ANOVA).

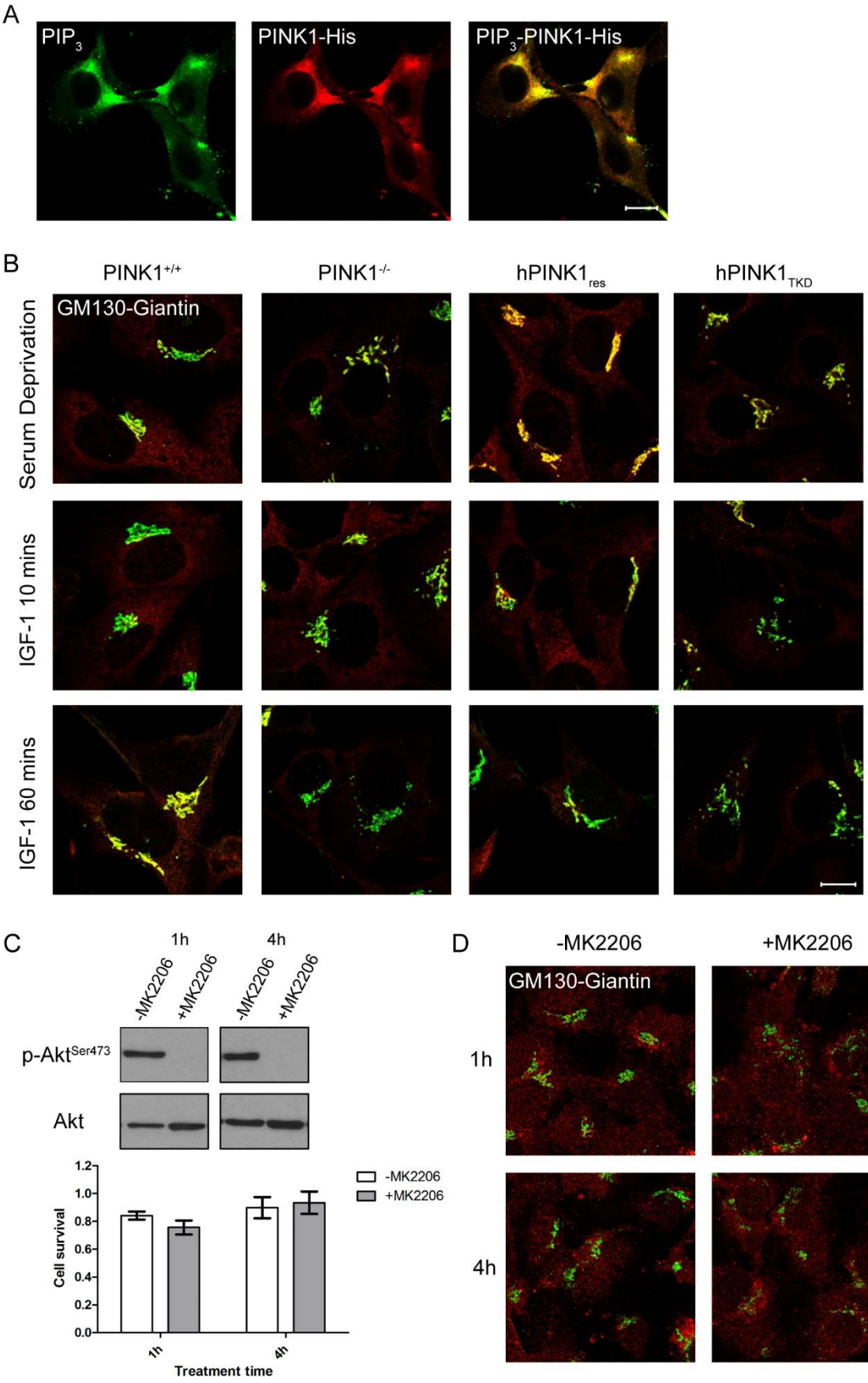

**Figure 6 PINK1 colocalises with $PIP_3$ and protects against Golgi fragmentation in an Akt dependent manner.**

A Representative confocal images showing $PIP_3$ colocalising with PINK1 in $hPINK1_{res}$ MEFs, which were grown in DMEM-Hi supplemented with 10% FBS, and stained with antibodies to $PIP_3$ (green) and His (red) (n = 3 biological replicates). Scale bar 10 μm. B Representative confocal images showing GM130 and Giantin localisation in $PINK1^{+/+}$, $PINK1^{-/-}$, $hPINK1_{res}$ and $hPINK1_{TKD}$ MEFs. Serum-starved cells were stimulated with 10 ng/ml IGF-1 for the indicated times, and immunostained for GM130 (green) and Giantin (red) (n = 3 biological replicates). Scale bar 10 μm. C Representative immunoblot analysis showing phosphorylation of Akt at $Ser^{473}$ and $Thr^{308}$ in $hPINK1_{res}$ MEFs incubated with 1μM MK2206 for the indicated times. Histogram depicting cell survival as measured by crystal violet staining in $hPINK1_{res}$ MEFs incubated with 1μM MK2206 for the indicated times. D Representative confocal images showing GM130 and Giantin localisation in $hPINK1_{res}$ MEFs. Serum-starved cells were incubated with 1μM MK2206 for the indicated times, and immunostained for GM130 (green) and Giantin (red) (n = 3 biological replicates). Scale bar 10 μm.

## Supplementary Materials and Methods

### RT-PCR

| Primer Set | Sequences | Conditions |
|---|---|---|
| mPINK1 | F: 5' GCTGATCGAGGAGAAGCAG 3'<br>R: 5' GATAATCCTCCAGACGGAAGC 3' | 95°C 15 min, [94°C 30 secs, 60°C 30 secs, 72°C 30 secs] 35 cycles. |
| hPINK1 | F: 5' AGACGCTTGCAGGGCTTTC 3'<br>R: 5' GGCAATGTAGGCATGGTGG 3' | 95°C 15 min, [94°C 30 secs, 50°C 30 secs, 72°C 30 secs] 35 cycles. |

## Supplementary Results

**Supplementary 1**

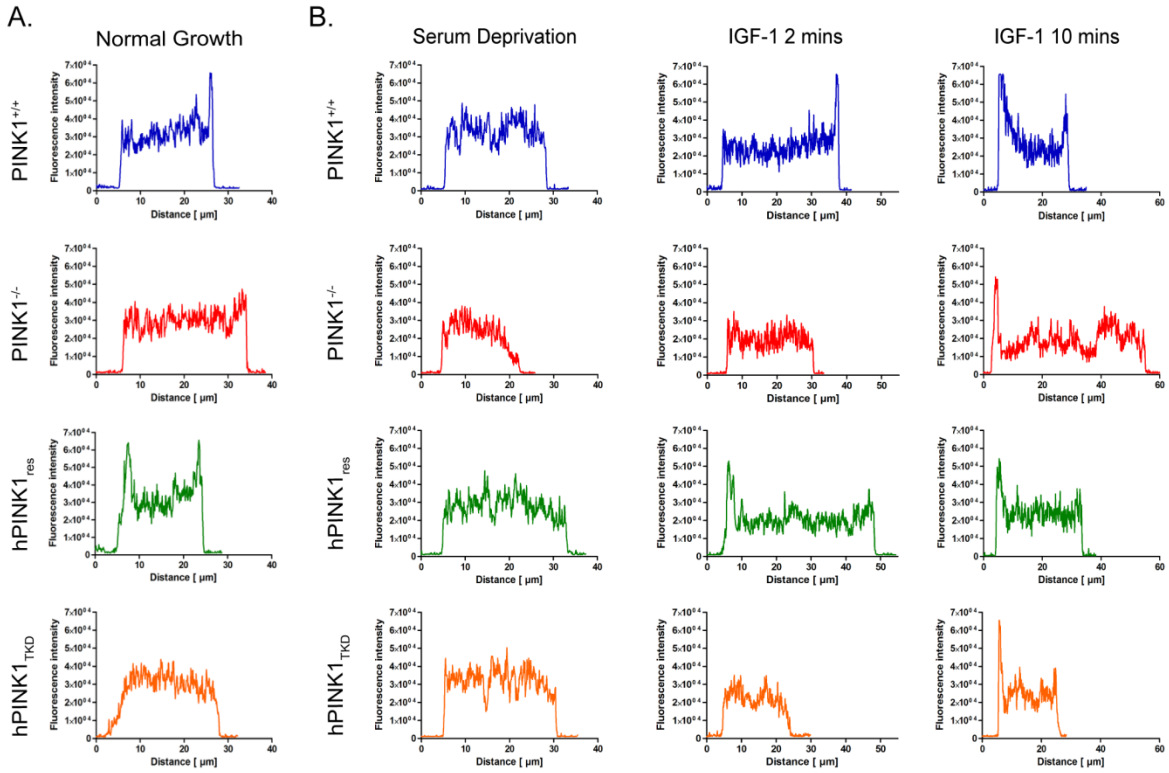


**Figure S1. Increases in fluorescence intensity at the plasma membrane show that PINK1 decreases the time taken for Akt localisation to the plasma membrane in response to IGF-1 stimulation.**

Representative line plots indicating the fluorescence intensity of GFP-Akt-PH along the white lines shown in Figure 2 (A) and 3 (A). Normal growth MEFs were grown in DMEM-Hi supplemented with 10% FBS. Serum-starved cells were stimulated with 10 ng/ml IGF-1 for the indicated times and subsequently stimulated with 10 ng/ml IGF-1. Scale bars 10 µm.

**Supplementary 2**

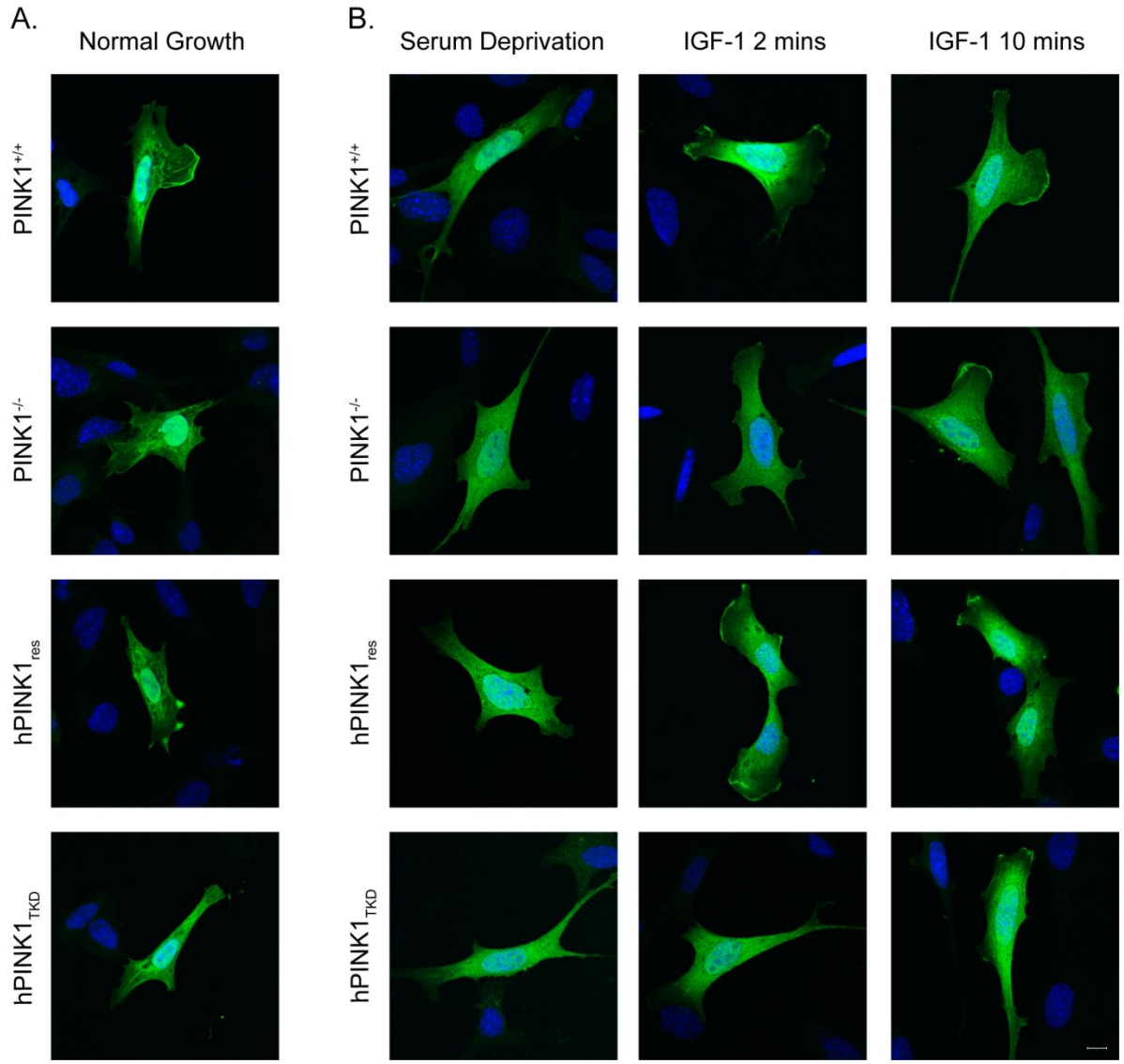


**Figure S2. PINK1 regulates the localisation of Akt to the plasma membrane under normal growth conditions and decreases the time taken for Akt to get to the plasma membrane in response to IGF-1 stimulation.**

A Representative confocal images showing GFP-Akt localisation in PINK1$^{+/+}$, PINK1$^{-/-}$, hPINK1$_{res}$ and hPINK1$_{TKD}$ MEFs, which were grown in DMEM-Hi supplemented with 10% FBS, transfected with GFP-Akt for 24h and stained with DAPI (blue). B Representative confocal images showing GFP-Akt localisation in PINK1$^{+/+}$, PINK1$^{-/-}$, hPINK1$_{res}$ and hPINK1$_{TKD}$ MEFs, following transfection with GFP-Akt for 24 h and stained with DAPI (blue). Serum-starved cells were stimulated with 10 ng/ml IGF-1 for the indicated times (n = 3). Scale bar 10 μm.

**Supplementary 3**

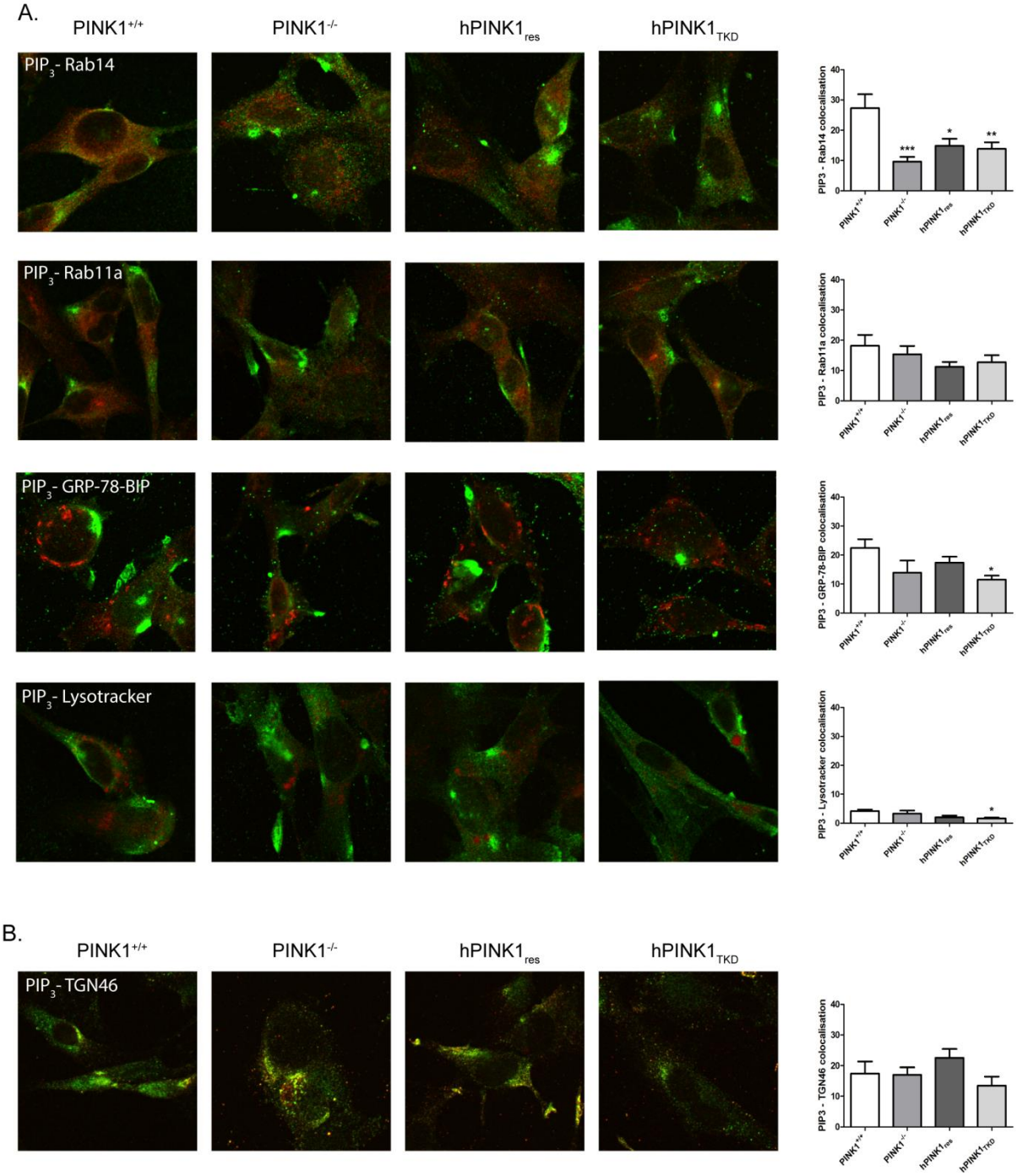


**Figure S3. Colocalisation analysis using endomembrane markers Rab14, Rab11a, GRP-78-BIP and Lysotracker reveals selective localisation of $PIP_3$ to the medial-Golgi.** Representative confocal images showing $PIP_3$ colocalisation with endomembrane markers in $PINK1^{+/+}$, $PINK1^{-/-}$, $hPINK1_{res}$ and $hPINK1_{TKD}$ MEFs, which were grown in DMEM-Hi supplemented with 10% FBS. A, B Cells were immunostained for $PIP_3$ (green) and Rab 14, Rab 11a, GRP-78-BIP, Lysotracker and TGN46 (red). Scale bar 10 µm. Data information: In A, B, data are presented in corresponding graphs as mean ± SEM (n=3 for each). *=$p < 0.05$, **=$p < 0.01$, and ***=$p < 0.0001$ with respect to $PINK1^{+/+}$ MEFs (One-way ANOVA).

**Supplementary 4**

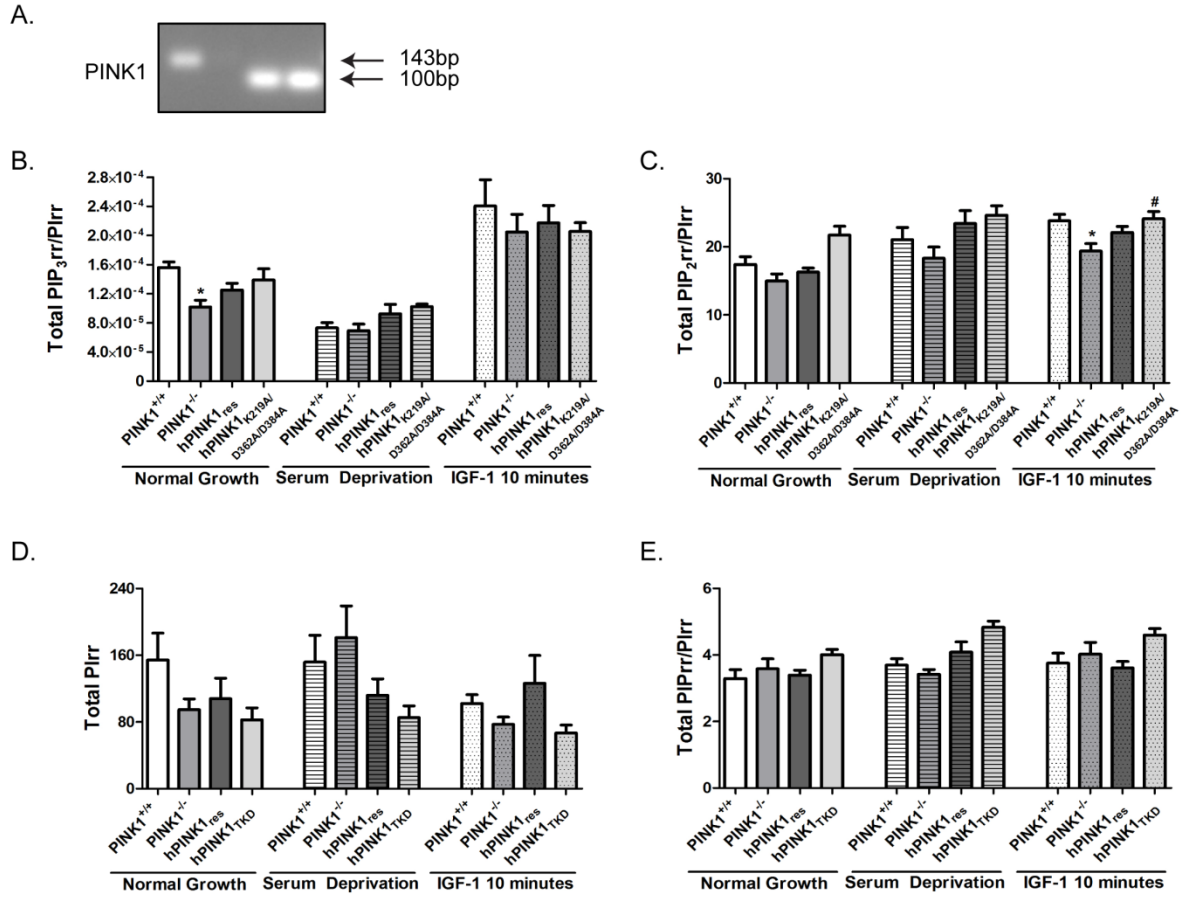


**Figure S4. PINK1 modification in MEFs, PINK1 modulates $PIP_3$ and $PIP_2$ levels.**

A. Agarose Gel showing PINK1 deletion and re-expression as confirmed by RNA extraction and RT-PCR analysis. Total $PIP_3$ (B), $PIP_2$ (C), PI (D), and PIP (E) levels as measured by mass spectrometry in $PINK1^{+/+}$, $PINK1^{-/-}$, $hPINK1_{res}$ and $hPINK1_{TKD}$ MEFs grown in DMEM-Hi supplemented with 10% FBS, serum deprived for 24h or stimulated with 10 ng/ml IGF-1 for 10 min (n = 3). Data information: In B-E, data are presented in corresponding graphs as mean ± SEM. *=$p < 0.05$ with respect to $PINK1^{+/+}$ MEFs, #=$p < 0.05$ with respect to $PINK1^{-/-}$ MEFs (Two-way ANOVA).

**Table S1. RT-PCR primer and conditions.**

| Primer Set | Sequences | Conditions |
|---|---|---|
| mPINK1 | F: 5' GCTGATCGAGGAGAAGCAG 3'<br>R: 5' GATAATCCTCCAGACGGAAGC 3' | 95°C 15 min, [94°C 30 secs, 60°C 30 secs, 72°C 30 secs] 35 cycles. |
| hPINK1 | F: 5' AGACGCTTGCAGGGCTTTC 3'<br>R: 5' GGCAATGTAGGCATGGTGG 3' | 95°C 15 min, [94°C 30 secs, 50°C 30 secs, 72°C 30 secs] 35 cycles. |

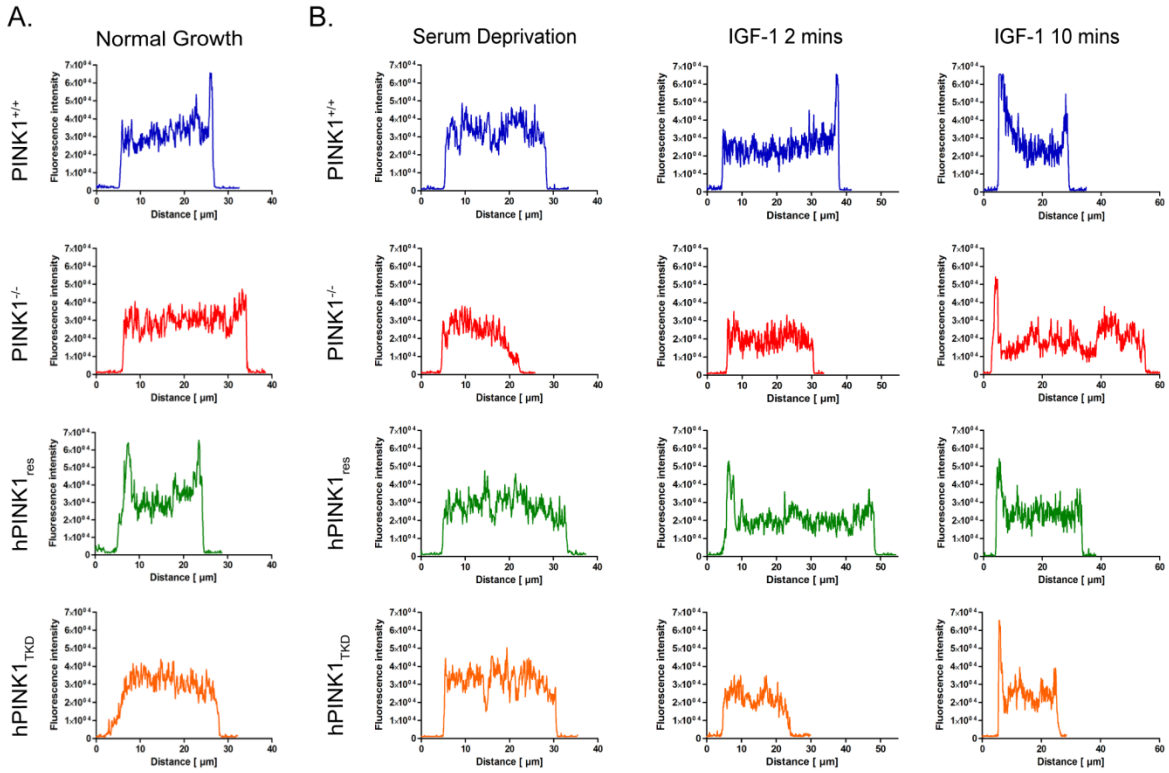


**Figure S1. Increases in fluorescence intensity at the plasma membrane show that PINK1 decreases the time taken for Akt localisation to the plasma membrane in response to IGF-1 stimulation.**

Representative line plots indicating the fluorescence intensity of GFP-Akt-PH along the white lines shown in Figure 2 (A) and 3 (A). Normal growth MEFs were grown in DMEM-Hi supplemented with 10% FBS. Serum-starved cells were stimulated with 10 ng/ml IGF-1 for the indicated times and subsequently stimulated with 10 ng/ml IGF-1. Scale bars 10 µm.

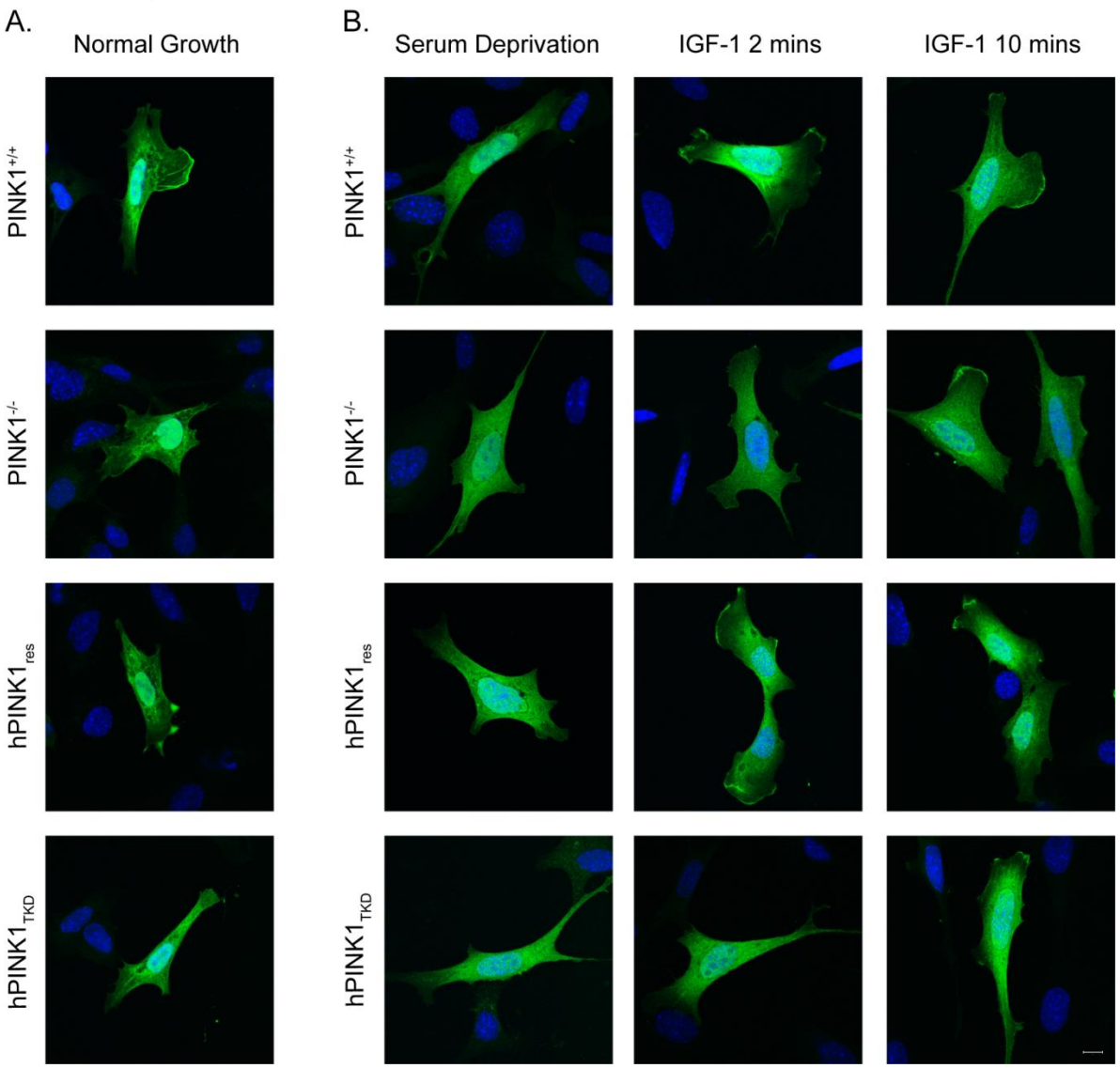


**Figure S2. PINK1 regulates the localisation of Akt to the plasma membrane under normal growth conditions and decreases the time taken for Akt to get to the plasma membrane in response to IGF-1 stimulation.**

A Representative confocal images showing GFP-Akt localisation in PINK1$^{+/+}$, PINK1$^{-/-}$, hPINK1$_{res}$ and hPINK1$_{TKD}$ MEFs, which were grown in DMEM-Hi supplemented with 10% FBS, transfected with GFP-Akt for 24h and stained with DAPI (blue). B Representative confocal images showing GFP-Akt localisation in PINK1$^{+/+}$, PINK1$^{-/-}$, hPINK1$_{res}$ and hPINK1$_{TKD}$ MEFs, following transfection with GFP-Akt for 24 h and stained with DAPI (blue). Serum-starved cells were stimulated with 10 ng/ml IGF-1 for the indicated times (n = 3). Scale bar 10 μm.

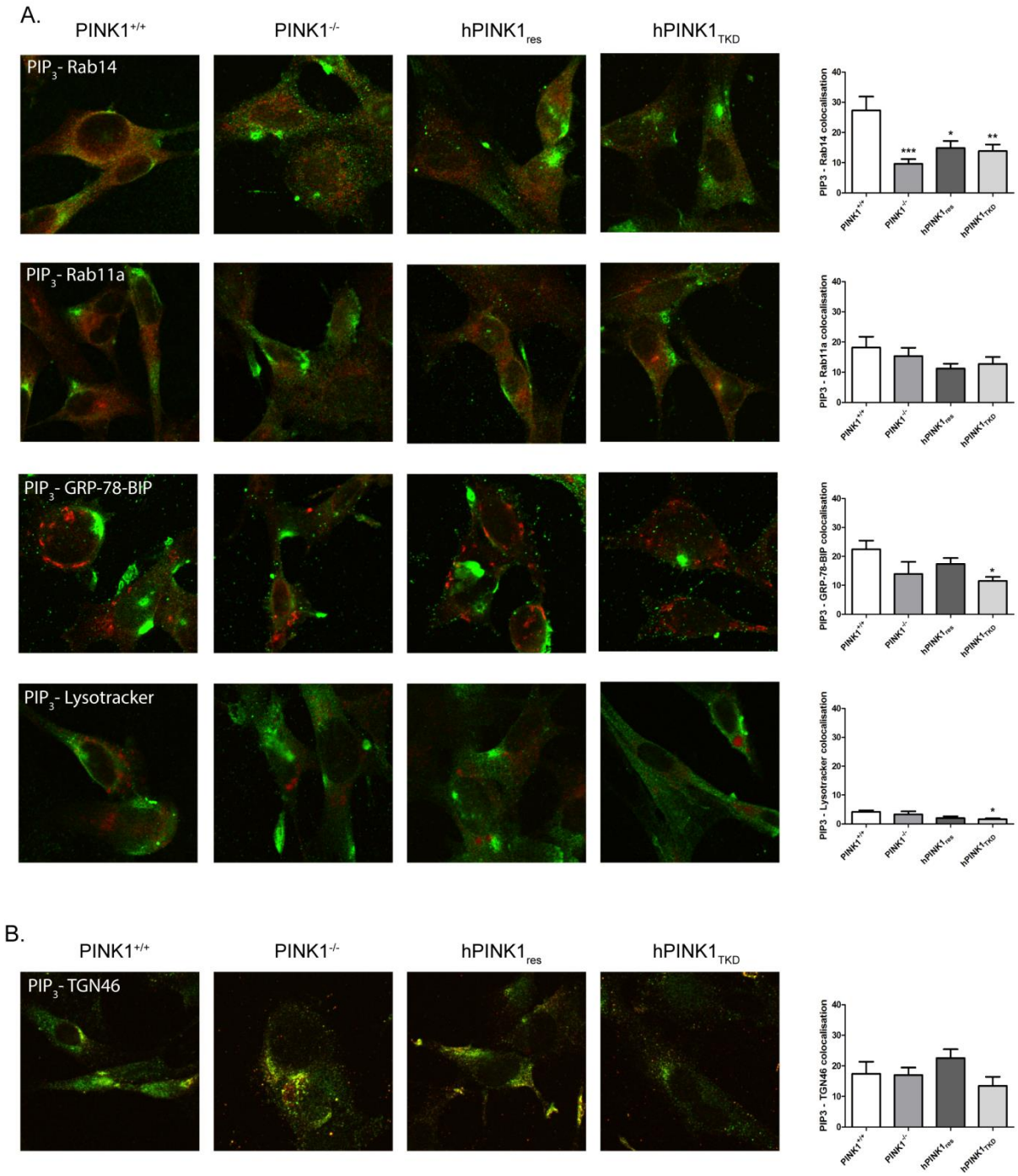


**Figure S3. Colocalisation analysis using endomembrane markers Rab14, Rab11a, GRP-78-BIP and Lysotracker reveals selective localisation of $PIP_3$ to the medial-Golgi.**

Representative confocal images showing $PIP_3$ colocalisation with endomembrane markers in $PINK1^{+/+}$, $PINK1^{-/-}$, $hPINK1_{res}$ and $hPINK1_{TKD}$ MEFs, which were grown in DMEM-Hi supplemented with 10% FBS. A, B Cells were immunostained for $PIP_3$ (green) and Rab 14, Rab 11a, GRP-78-BIP, Lysotracker and TGN46 (red). Scale bar 10 µm. Data information: In A, B, data are presented in corresponding graphs as mean ± SEM (n=3 for each). *=$p < 0.05$, **=$p < 0.01$, and ***=$p < 0.0001$ with respect to $PINK1^{+/+}$ MEFs (One-way ANOVA).

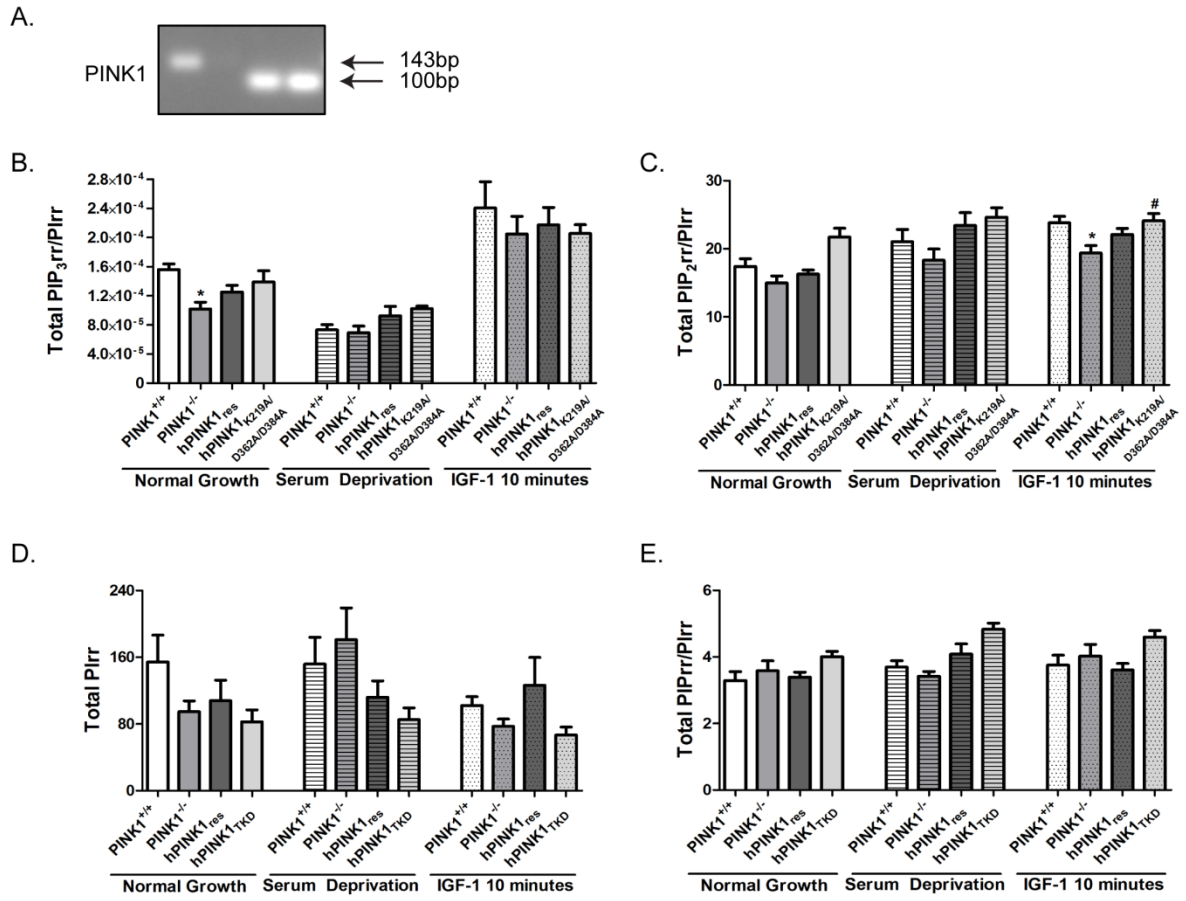


**Figure S4. PINK1 modification in MEFs, PINK1 modulates $PIP_3$ and $PIP_2$ levels.**

A. Agarose Gel showing PINK1 deletion and re-expression as confirmed by RNA extraction and RT-PCR analysis. Total $PIP_3$ (B), $PIP_2$ (C), PI (D), and PIP (E) levels as measured by mass spectrometry in $PINK1^{+/+}$, $PINK1^{-/-}$, $hPINK1_{res}$ and $hPINK1_{TKD}$ MEFs grown in DMEM-Hi supplemented with 10% FBS, serum deprived for 24h or stimulated with 10 ng/ml IGF-1 for 10 min (n = 3). Data information: In B-E, data are presented in corresponding graphs as mean ± SEM. *=$p < 0.05$ with respect to $PINK1^{+/+}$ MEFs, #=$p < 0.05$ with respect to $PINK1^{-/-}$ MEFs (Two-way ANOVA).